

1 Introduction

1.1 Equilibrium Morphology

Coastal and river systems including beaches and tidal inlets evolve naturally and adapt to their forcing conditions, often forming stable shapes or equilibrium morphologies if the conditions persist over a period of time. The placement of some structures on a beach can lead to the formation of a new equilibrium position. Similarly the positioning of bridge piles or culverts in rivers can lead to the rearrangement of sediment and the development of a new equilibrium morphology. It is of interest to managers and planners to be able to predict what would happen to the morphology if these conditions changed. A change in conditions may include the placement of a detached breakwater parallel to the shoreline, or the installation of groynes to help stabilise beaches. Examples of potential equilibrium morphologies associated with these structures can be seen in Figure 1.1 and Figure 1.2.

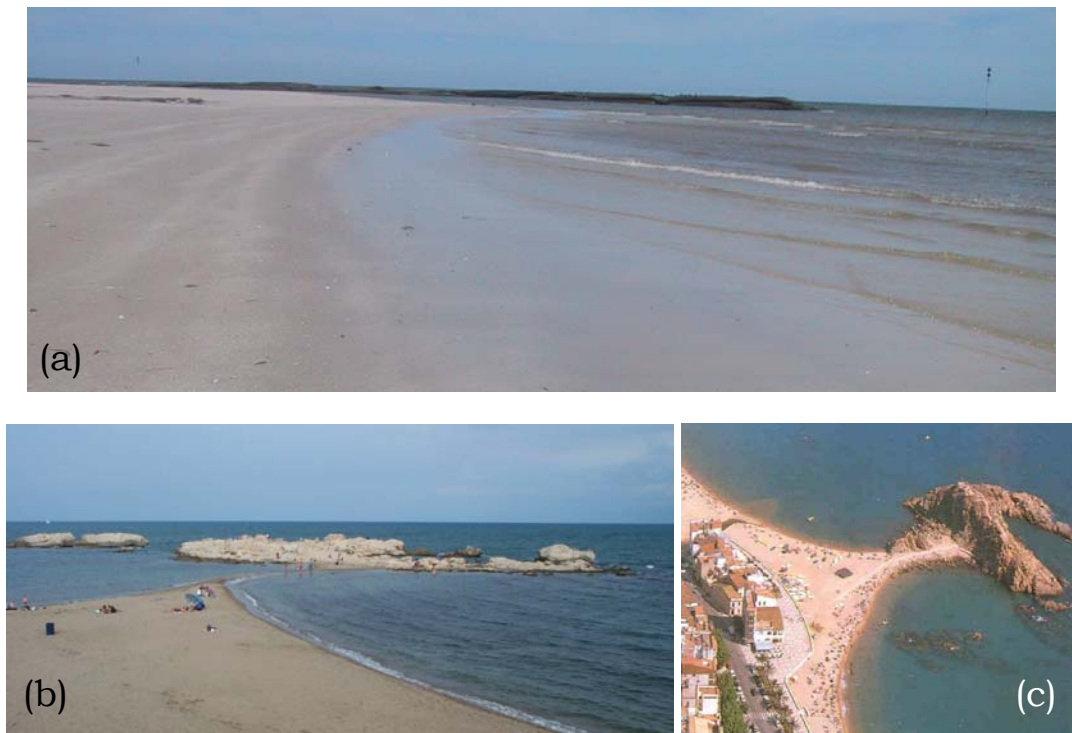


Figure 1.1 Examples of equilibrium morphologies that form in the lee of breakwaters. (a) Semaphore Beach, Adelaide, Australia, (b) Costa Brava, Spain, (c) Blanes, Spain.

Similar to beach morphologies, different river flow patterns through a tidal inlet or sandy lagoon, and the interaction of the ocean with these flows, can lead to the development of complex equilibrium morphologies when the conditions

remain similar for a period of time. Complex morphologies such as those associated with tidal inlets can be hard to predict in the medium- and long-term. Medium-term modelling is defined as the changes that occur over weeks and months while long-term predictions make suggestions as to the morphology that will result after years and decades (Southgate, 1995). Examples of complex tidal inlet morphologies are shown in Figure 1.3.

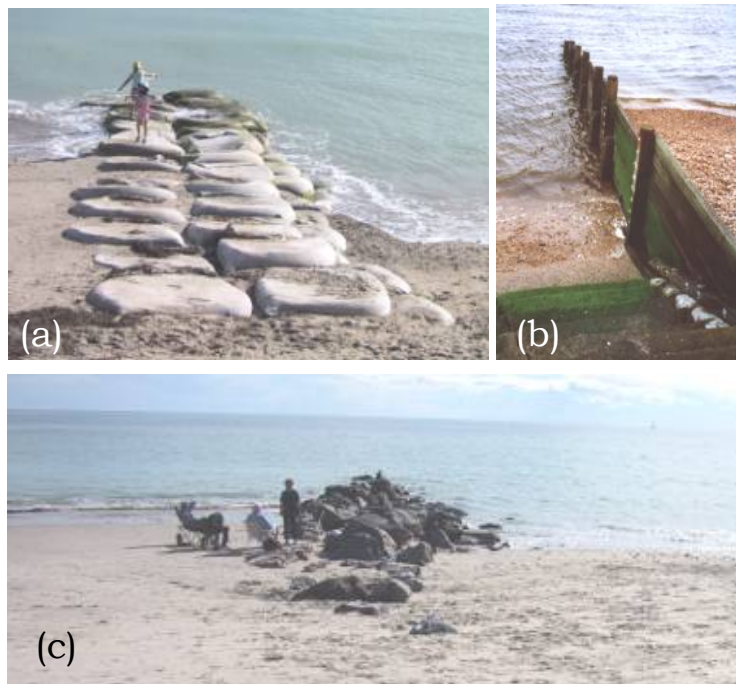


Figure 1.2 Examples of equilibrium morphologies that form due to groyne placement. (a) Somerton Beach, Adelaide, Australia, (b) Herne Bay Beach, Kent, UK, (c) Glenelg Beach, Adelaide, Australia.



Figure 1.3 Examples of equilibrium morphologies associated with different river flow and tidal conditions through a tidal inlet at the Murray Mouth, South Australia during 1980 and 2000.

More research on the evolution of estuaries is required to enable a better understanding of the processes that form them and allow for their adequate environmental management (Kench, 1999). Blondeaux (2001) agrees that in general, more research into the development of models capable of determining long-term coastal morphological evolution is needed.

1.1.1 Traditional Modelling Methods

In general, predictions are typically made by traditional process-based models, where wave, current, sediment transport and sediment balance modules are evaluated on a time stepping basis for a period of time until the changes between steps become slight and a near equilibrium morphology is formed (de Vriend et al., 1993; Nicholson et al., 1997; Leont'yev, 1999; Zyserman and Johnson, 2002).

When two-dimensional, depth averaged (2DH) models are applied over an extended period of time, complications may result due to the use of time stepping, particularly in complex systems such as those associated with tidal inlets (de Vriend et al., 1993; Southgate, 1995; Reeve and Fleming, 1997; Dodd et al., 2003; Hanson et al., 2003; Southgate et al., 2003; Aagaard et al., 2004; Różyński, 2005). For example, if a small anomaly occurs during one time-step, even though initially the difference from the actual morphology may be minor, the anomaly can propagate through the solution, become amplified, and lead to a nonsensical morphology (Reeve and Fleming, 1997; Hanson et al., 2003).

Alternatively, if there is a minor error in initial conditions, the solution may move to an incorrect morphology (de Vriend et al., 1993; Southgate, 1995; Sloff et al., 2004). Sloff and colleagues found this when they tried to model a laboratory experiment where a channel formed in a wide, sand covered flume, with narrow entrance and exit channels at either end. Only a slight difference in initial conditions in their computer model made the channel form on the opposite side of the flume to that observed in the laboratory experiments. This was not observed in the laboratory experiment where the channel always formed on the same side. This is diagrammatically shown in Figure 1.4.

Time-stepping models do not have the ability to compare different pathways and scenarios. Once the flow starts moving sediment in one direction, it will continue on that path. It is not possible to step back and examine a number of different possibilities that are not associated with the fixed initial conditions. The fixed initial conditions may have accumulated errors during the measurement process. The work proposed in this thesis is not as dependent on initial conditions

because equilibrium morphologies are compared directly, thereby reducing the potential for anomaly amplification as the intermediate time-steps are eliminated.

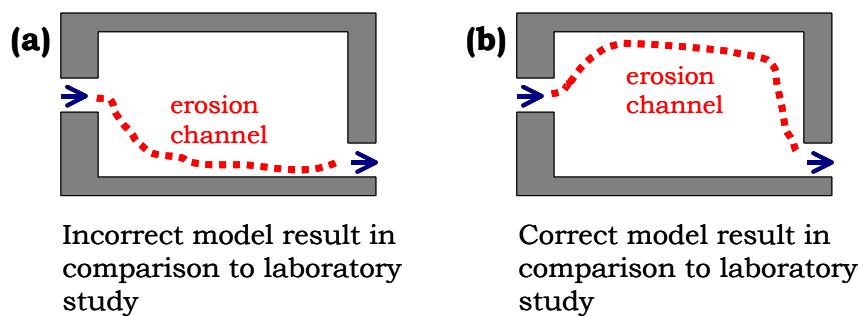


Figure 1.4 Example from Sloff et al. (2004) of slightly different initial conditions producing a completely different modelling result, with a channel forming on the opposite side of the flume to that observed in laboratory experiments.

1.2 Aims

The primary aim of this research was to develop a number of alternative approaches to traditional process-based models, able to predict medium-term equilibrium morphologies.

To validate these alternative approaches, the developed models were applied to a number of case study examples, making comparisons between experimental results and conventional models, both qualitatively and quantitatively.

1.2.1 Development of New Modelling Methods

In this thesis, non-conventional methods that are not time-step based have been proposed to predict equilibrium morphologies. Two different methods have been developed.

Firstly a self-organisation-based method was formulated. Self-organisation can be demonstrated by the application of simple rules in a cellular automata type model, where the local rules affect sediment movement to the cells immediately surrounding the target cell. Through positive and negative feedback associated with local cell interaction, a global stable shape results. Self-organisation methods have been applied to explain a myriad of coastal formations including cusps (Coco et al., 2004), ripples (Pannell et al., 2002), nearshore crescentic and transverse sandbars (Caballeria et al., 2002) and sorted sediment patterns on shallow continental shelves (Murray and Thieler, 2004).

Following on from the use of self-organisation, an entropy-based method was also developed. This entropy-based method was inspired by work undertaken in the field of river morphology, first initiated over 40 years ago by Leopold and Langbein (1962). A system attains equilibrium when its entropy production is a minimum in the case of open systems (Prigogine, 1967). This pertains to a state where energy dissipation is minimised, as, if the entropy production is minimised, the energy dissipated to increase the entropy must also be at a minimum (Yang, 1994). Since the pioneering efforts of Leopold and Langbein, a number of theories related to minimum energy dissipation have been applied in the prediction of optimal channels and river networks (Rodríguez-Iturbe et al., 1992; Maritan et al., 1996; Banavar et al., 1997; Cleveringa et al., 1997; Molnár and Ramírez, 1998; Rinaldo et al., 1998; Rinaldo, 1999; Molnár and Ramírez 2002).

These entropy-based river methods have had little transference into the field of coastal morphological modelling. Wright et al. (1973) undertook a study using uniform work as a basis for describing the planforms of a number of estuaries in the field. Their work was mainly theoretically based, which is a trait common to a lot of work with entropy-based principles, possibly due to lack of computational power and suitable global optimisation routines. The work in this thesis expands on previous theoretical research and large-scale one-dimensional or planform examples, predicting complex morphologies in detail over relatively compact areas.

1.2.2 Case Studies

In this thesis the methods described above, and the resulting models, have been applied to a number of case studies to test their predictive abilities.

Firstly, laboratory-sized constriction and obstruction examples were considered for the application of the self-organisation-based modelling method. These case studies are pictured in Figure 1.5, and consisted of unidirectional flow through a long rectangular flume. The flow was controlled to produce conditions that enabled clear-water scour in the vicinity of the obstruction or constriction, but allowed the bed to remain unchanged elsewhere in the flume. In general, areas of erosion occurred in the throat of the constriction and between the obstruction and flume walls, while deposition occurred downstream of these scour holes.

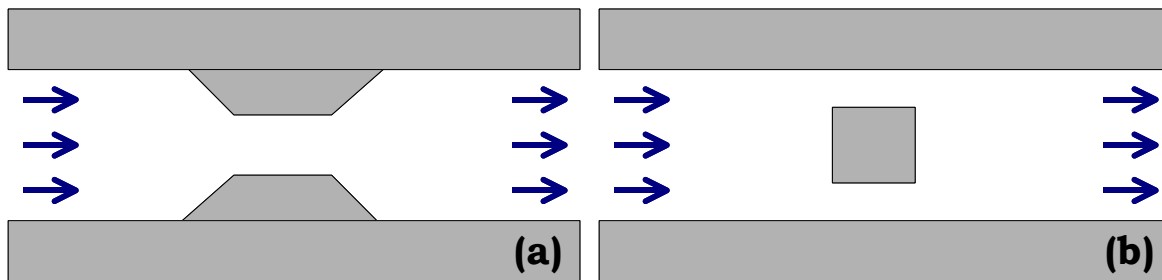


Figure 1.5 Examples of the (a) constriction and (b) obstruction laboratory case studies to which the self-organisation based model was applied.

The constriction and obstruction examples were chosen as they represented situations easily constructed and controlled in the laboratory, whilst representing common field conditions such as scour around bridge piers. The benefit of undertaking laboratory experiments was that they could be analysed in a controlled environment, with known initial and final bed morphologies, velocities and flow rates.

Secondly, a number of laboratory- and field-sized case studies were explored, examining the equilibrium morphologies that could be predicted using the self-organisation-based and entropy-based models for a sandy lagoon/inlet with both inflow and outflow channels. These case studies are pictured in Figure 1.6. Again, only clear-water scour was considered, with unidirectional flow creating erosional channels between the flow entrance and exits in the majority of cases.

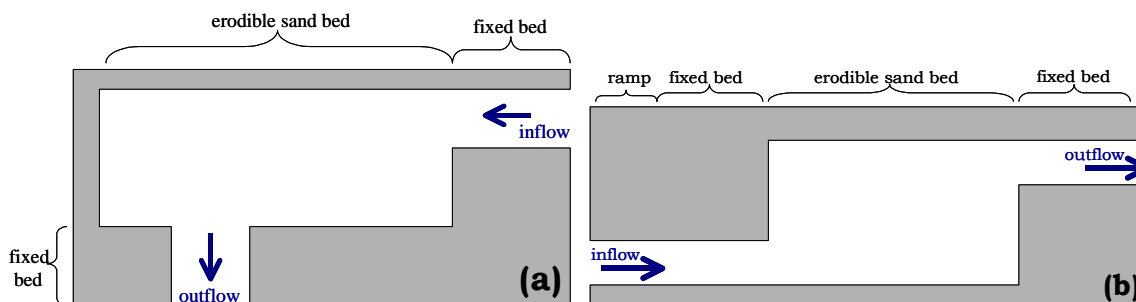


Figure 1.6 Examples of the unidirectional sandy lagoon of (a) field sized and (b) laboratory sized case studies to which the self-organisation-based and entropy-based models were applied.

These case studies were chosen as they represented a simplified situation of complex coastal environments such as those mentioned in Section 1.1.1 and pictured in Figure 1.3. They expanded on the typical case studies to which entropy-based models are generally applied to, which involve large-scale, one-dimensional or planform river longitudinal profiles or networks. They involve a fixed area with a controlled entrance and exit to allow ease of comparison

between predicted morphologies. The laboratory-sized experiment was also able to be easily undertaken in a controlled environment with known initial and final bed morphologies, velocities and flow rates that allowed flow to erode a channel for a sufficient period of time for an equilibrium morphology to be observed.

Lastly, as an extension from entropy-based modelling, objective functions based on sediment transport minimisation were proposed for complex coastal environments, such as the prediction of the equilibrium morphology that forms in response to a shore parallel breakwater.

An offshore breakwater was chosen as the case study subject for this research as it is a typical situation where stable, predictable equilibrium morphologies evolve in the field. It is also an area where equilibrium prediction comparisons have been made in the past using conventional models (Nicholson et al., 1997; Zyserman and Johnson, 2002).

1.2.3 Differences Between the New and Traditional Modelling Methods

The entropy-based model is strikingly different from a traditional model. It can start from a random morphology, with perturbations made to the initial morphology. In contrast, conventional models generally start with a single initial morphology. The entropy-based model then uses optimisation techniques to compare and modify a specified number of random morphologies, gradually pinpointing the one that reduces the objective function to a near minimum value. Snap shots of morphologies are compared with each other to see which is closer to equilibrium, rather than following the process of sand transport step-by-step.

The entropy-based method approaches morphological modelling from a different angle. It assumes that equilibrium morphologies develop when stable conditions exist for a period of time. It pinpoints the characteristics that define equilibrium and exploits these characteristics, using them to determine whether a certain morphology is close to equilibrium. In contrast, conventional models move sediment on a step-by-step basis, and arrive at an equilibrium situation when sediment is no longer actively moved around the system.

1.3 Research Outline and Approach

Research into alternative morphological modelling methods has been undertaken in a number of stages, the results of which are set out in this thesis. Firstly, a description of the inspiration for this work, and research that forms a basis for

the current study are discussed and compared at length in Chapter Two. The past uses of both self-organisation and entropy-based models are discussed and the links exposed and gaps covered in this thesis are defined.

The general method developed for the self-organisation-based cellular automata model is explained in Chapter Three, followed by its application to the equilibrium morphologies that develop due to unidirectional flow around solid constrictions and obstructions. Some quantitative comparisons are made. These comparisons contrast the ability of the self-organisation-based method to make predictions of equilibrium morphologies measured in a number of laboratory experiments against results obtained using a more traditional model. Traditional process-based model results are documented, and quantitative comparisons made with the equilibrium morphologies measured during a number of laboratory experiments. The Brier Skill Score is used for these quantitative comparisons, with the self-organisation-based model performing favourably.

The second part of Chapter Three expands on the laboratory-sized analyses and applies a self-organisation model to a unidirectional sandy lagoon with a scale of kilometres. The energy dissipation from the system, as the system self-organises and develops a stable morphology, is recorded. The energy dissipation trend is then linked to entropy-based research, where an open system is defined as reaching an equilibrium morphology when its energy dissipation is minimised. This leads to the development of entropy-based modelling in Chapter Four.

Chapter Four utilises the knowledge found from the self-organisation modelling to develop an optimisation-based model, the method of which is explained in detail. Special attention is given to the documentation of the development of an effective optimisation routine, needed for use in conjunction with the entropy-based method. It includes results from a number of tests, using the global optimisation techniques to define flow fields around an obstruction in a channel. The optimisation routines are then utilised in the detection of optimal channel morphologies that form through an erodible bed unidirectional lagoon system, similar to the one considered in Chapter Three. This entropy-based model minimises energy dissipation in the system both locally and globally, with the use of genetic algorithms (GAs) and simulated annealing (SA) to predict an equilibrium morphology resembling that found in the field. This work is then expanded, considering a lagoon system with reversing flow.

A sandbox experiment in the laboratory was then performed, on a much smaller scale than the lagoon simulations. The entropy-based method is able to correctly

predict the erosion channel, with a greater accuracy than a comparable conventional model.

In Chapter Five, the use of optimisation to predict equilibrium morphologies is examined with respect to coastal environments, where regular waves attack a shore parallel breakwater. Optimisation is utilised, in conjunction with a suitable objective function based on sediment transport minimisation, to immediately predict equilibrium morphologies. This eliminates the need for intermediate morphologies. This method is applied to a field scale example.

Chapter Six summarises the research presented in this thesis. It highlights the relevance and implications of the research and makes suggestions on areas of further research.

2 Literature Review

It is imperative to have the ability to predict morphologies at equilibrium, to assist with the design and management of structures such as breakwaters, groynes and bridges, as well as the management and maintenance of estuaries, tidal lagoons and river systems. This Chapter outlines current modelling methods, their gaps and weaknesses and the potential to develop new modelling methods. Two alternative methods are analysed, based on entropy principles and self-organisation.

Entropy-based methods that have been used in river morphodynamic modelling are discussed, in particular the minimum rate of energy dissipation. These methods have been used to model the longitudinal profiles of rivers and dendritic river networks (Leopold and Langbein, 1962; Rodríguez-Iturbe et al., 1992). A short discussion is included on two global optimisation methods: genetic algorithms and simulated annealing. These methods are of use when a minimum objective function must be found to determine an equilibrium or stable morphology in conjunction with entropy-based methods.

Models using self-organisation are now emerging as a simple and effective way to predict stable patterns in fields such as fluvial geomorphology and ripple formation. They have been used to model systems that include beach cusps and longshore bars as well as drainage networks (Hergarten and Neugebauer, 2001; Caballeria et al., 2002; Coco et al., 2004). A description and discussion of these methods is given in this Chapter.

Finally, the Chapter ends with a summary of the gaps in the literature that can be exploited, and areas that have inspired the research presented in this thesis.

2.1 General Modelling Methods Currently Used For Medium- and Long-Term Predictions

Environments such as groyne fields, offshore breakwaters, jetties and tidal lagoons, as well as scour in river beds associated with river engineering structures such as bridge piers, all require accurate morphological predictions in order to facilitate their design and management. Typically, conventional process-based models are employed for this purpose.

Process-based models used for medium-term predictions in coastal environments usually incorporate a number of separate modules that deal with sediment transport, wave field determination, current field determination and sediment

balance, as is shown in Figure 2.1 (de Vriend et al., 1993; Nicholson et al., 1997; Leont'yev, 1999; Zyserman and Johnson, 2002; Sutherland et al., 2004). Conventional models work by stepping through time. With each time step, a new bathymetry is formed after wave, current, sediment transport and sediment balance modules are all applied to the previous bathymetry. The system is defined as reaching equilibrium when the formation that results becomes stable, and does not change with successive time-steps.

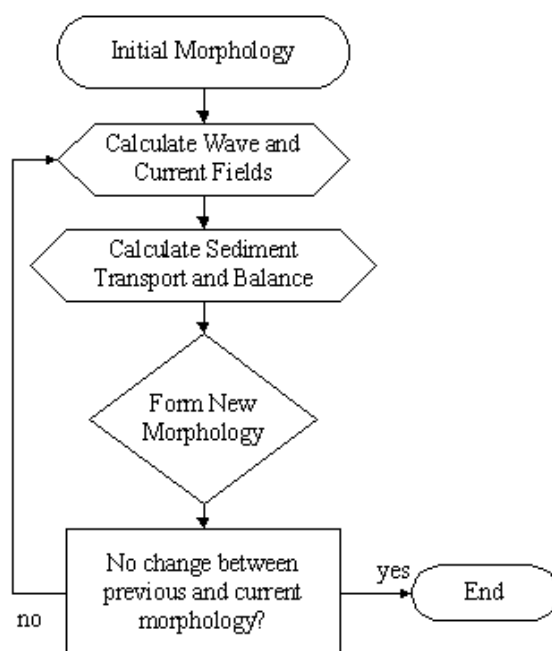


Figure 2.1 General conventional process-based coastal model structure for predicting morphologies at equilibrium.

Process-based models have some possible limitations where medium-term or long-term predictions of complex morphologies such as those associated with tidal inlets are required (de Vriend et al., 1993; Southgate, 1995; Ruessink and Terwindt, 2000; Stive et al., 2002; Hanson et al., 2003; Witting and Zanke, 2004). If a small anomaly in prediction occurs over a single time-step, the effect is of no great consequence, however, over many time steps, it can be amplified to a size that affects the end morphological prediction (Reeve and Fleming, 1997; Hanson et al., 2003). This and other potential problems associated with process-based models are elaborated on in Section 2.1.1.

In the field of river morphology, researchers have avoided the time-stepping process, by jumping to an equilibrium morphology directly, using entropy-based principles to define a stable system (Yang, 1971; Huang et al., 2004). These methods are discussed in Section 2.2. This Section briefly describes some of the current research into the prediction of medium- and long-term coastal

morphologies. Self-organisation-based methods, an emerging form of modelling rhythmic repetitive coastal features, are discussed later in Section 2.4.

In general, large-scale coastal modelling is performed by either process-based models, where short-term processes are used to develop a morphology over time, model reduction methods, where processes are rescaled and their integrated effect is considered, or behaviour-orientated models, where the physical processes are ignored, in favour of the observed response of the landscape (de Vriend et al., 1993; Jiménez and Sánchez-Arcilla, 2004). Jiménez and Sánchez-Arcilla (2004) developed a hybrid process-based behaviour one-line model, that utilised averaged wave conditions and a long-term parameterised longshore sediment transport rate to make predictions on the long-term evolution of a barrier coast system. They were able to predict the coastline movement observed at the Ebro Delta, Spain, but their model was of one-line dimension, and the development of a model capable of predicting complete three-dimensional morphology in the near-shore zone would be beneficial. Falqués and Calvete (2005) used stability analysis with an extended one-line model to analyse long-term dynamics of the shoreline. Their extended model accounted for the variation of wave height and angle at breaking due to the different positioning of the shoreline, by utilising an equilibrium cross-shore profile that extended from the points on their one-line model. This was an improvement over a one-line only model, but still did not encompass the full three-dimensional aspect of the nearshore zone morphology.

To avoid some of the limitations associated with process-based models, Stive and de Vriend (1995) used a behaviour-orientated model to make shoreface profile predictions. Stive et al. (2002) took a similar approach, qualitatively classifying the evolution of the Dutch coast and pointing out the benefits of ARGUS image assimilation in the modelling of medium- and long-term morphological phenomenon. This is useful to give a qualitative insight into what might be expected in the evolution of certain environments, but a quantitative model would be even more beneficial. The reliance on behavioural models is limited by the availability of good field observational data, while process-based models can apply knowledge of similar acting processes to different situations. Field data is expensive to obtain and the ability to be able to model an area with limited or inferred data is beneficial. Stive et al. (2002) mentioned however, that a better understanding of the underlying principles is needed in order to give better predictions using numerical models.

Morphological models tend to be as reliable as the theory and implementation of the individual processes involved. The representation of individual processes is

limited by current knowledge of these nearshore processes. Long computation time also limits process representation as the more detailed a process, the longer the runtime. For example a quasi three-dimensional flow model would take longer to run than a two-dimensional, depth-averaged model. In situations where long-term modelling is required, the computation time required can become excessive depending on the complexity of both the model and system.

Local sand transport processes have the greatest effect on coastline evolution, and unfortunately there is still a lack of well-validated and reliable methods for sediment transporting processes (Davies et al., 2002). More research is needed in the sediment transport area to improve the fundamental knowledge and modelling of these sand transport processes and hence improve their representation in process-based models. A model method with a greater reliance on a poorly validated sediment transport model routine will not predict as accurate a morphology as a model less reliant on sediment transport in its overall morphological predictions.

Models can be one-, two- or three- dimensional, but due to the complexity involved with three-dimensional modelling, two-dimensional modelling is more commonly used. Most two-dimensional models have a fixed bottom step (de Vriend, 1987). This means that the bottom is kept constant while water and sediment movements are calculated, after which a change-in-bottom-step module is performed, with water and sediment movement kept constant. This creates a one-way system, without feedback in the first step. However, it does reduce run times.

Kobayashi and Johnson (2001) and Kobayashi and Tega (2002) overcame some of the problems of long runtimes by their use of a one-dimensional time-dependent model. They determined equilibrium beach profiles in the surf and swash zones by predicting temporal and spatial variations of depth-averaged sediment concentrations. This modelling method also overcame the problem of inaccuracy in two-dimensional models due to a limited knowledge of bottom boundary layer sediment dynamics. Kobayashi and Johnson (2001) were able to predict both accretion and erosion accurately, an improvement over other models which were better at predicting one or the other. However, as with other process-based models, Kobayashi and Johnson's model is liable to cause an amplification of anomalies when run for a long simulation period due to the nature of the time-stepping process.

Zyserman and Johnson (2002) developed a quasi-three-dimensional (Q3D) process-based model, where the sediment transport and mean flow were

described in three-dimensions. Their model was used to predict equilibrium formations behind detached breakwaters. Empirical as well as two-dimensional-horizontal (2DH) models and field observations predicted similar planform shapes to the Q3D model. The developed model predicted realistic morphologies but still had the potential for anomaly amplification or excessive computational time. A model that utilised the quasi-3D calculations to predict equilibrium morphologies directly without the need to time-step would reduce the potential for this type of problem to occur.

Nicholson et al. (1997) compared five different process-based 2DH models, all of which used slightly different ordering and equations, but included the basic modules as outlined in Figure 2.1. All models gave the same basic quantitative result, but there were many differences when the fine detail was analysed. The use of different sediment transport formulae had a large effect on the equilibrium planform shape, determining whether a salient or tombolo formed. The type of wave used, be it regular or irregular, also had a considerable effect on the resultant morphology. In general, the overall morphologies predicted by the models were in agreement with laboratory and field study results. The other difference found highlights potential problems associated with the use of different equations and ordering of modules.

Nicholson et al. (1997) suggested that feedback between hydrodynamic and morphologic modules was very important. Self-organisation is a methodology based around feedback and is discussed in detail in Section 2.4 as an alternative to current morphological prediction models.

2.1.1 Process-Based Models and Their Potential Limitations

Process-based models have a number of potential problems associated with them as discussed by de Vriend et al. (1993). These traditional modelling methods have a poor representation of nonlinearity meaning that they cannot accurately represent systems over long timescales (Southgate, 1995; Reeve and Fleming, 1997; Dodd et al., 2003; Southgate et al., 2003; Aagaard et al., 2004; Różyński, 2005). This means that if a small anomaly occurs during a single time-step, the perturbation may propagate through the solution, become amplified and result in a large error in the end morphological prediction (Reeve and Fleming, 1997; Hanson et al., 2003).

Another problem associated with traditional modelling methods is the large amount of computational time required to model medium and long term equilibrium morphologies of complex systems (de Vriend et al., 1993; Stive and

de Vriend, 1995; Reeve and Fleming, 1997; Nicholas, 2005; Willgoose, 2005). In some instances it may take one hour to run a simulation of four hours. If a long-term prediction is undertaken, the time requirements will become uneconomical. Conventional methods are limited by the linear nature of time stepping and are unable to avoid the need to time-step by predicting equilibrium morphologies directly, thereby reducing computational time.

The need to specify starting and driving conditions is another problem of process-based models (de Vriend et al., 1993). Sloff et al. (2004) observed that their numerical model of channel formation in a wide reservoir was very dependent on the initial conditions and boundary conditions that were specified. An example of the results they obtained in their laboratory study is given in Figure 2.2. If the exact combinations were used, the process-based model could be made to agree with laboratory observations. If the conditions were only slightly wrong, a different morphology resulted. In the case of the Sloff and colleagues experiment, the channel formed on the right side of the flume instead of the left side (the direction is taken looking down the flume in the direction of flow). Sloff et al.'s (2004) model was reliant on initial conditions. It was not able to compare a number of different scenarios, quasi-independent of initial conditions, to decipher which was closer to equilibrium.

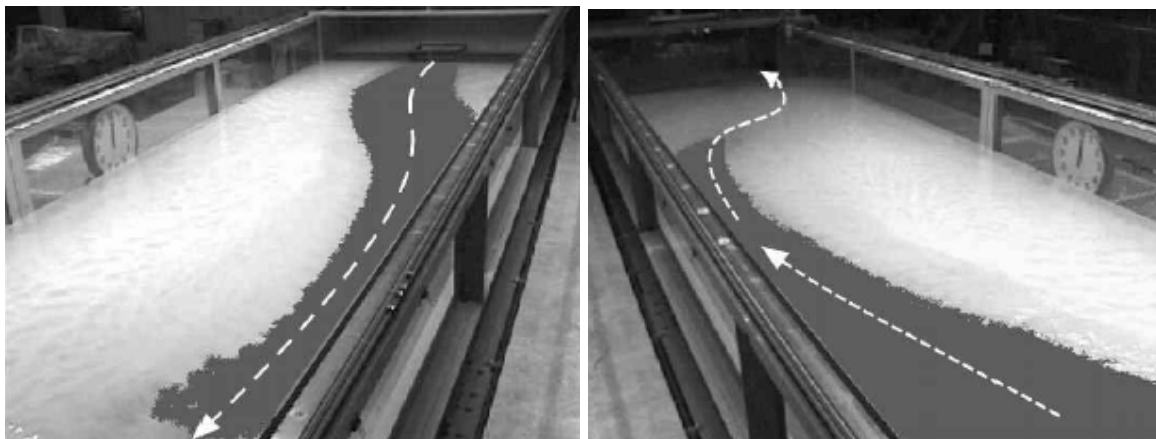


Figure 2.2 Laboratory results obtained in a wide reservoir study (after Sloff et al., 2004).

The same problems associated with sensitivity to initial conditions also apply to the application of driving conditions. If driving conditions are incorrect or even applied in the wrong order, errors may occur in the equilibrium morphology prediction (Southgate, 1995). Southgate found that the order that waves were applied in a medium-term model was important in determining the end morphology. The importance decreased however if the last applied condition was strong and therefore imparted a greater influence on the morphology. For

example, if a storm event occurs at the end of a wave sequence, the waves are more likely to mould the bed to the observed equilibrium morphology. If a sequence of smaller wave events are applied, with less potential to create a large impact on the remoulding of the bed, the sequence these small events are applied in has more of an effect as to whether the sand is in a certain position and able to be moved.

Ruessink and Terwindt (2000) suggested that the influence of feedback between hydrodynamics and morphology meant that the wave chronology and initial conditions were not as important for medium-term predictions. They used a probabilistic wave model to predict the qualitative behaviour of nearshore bars. Payo et al. (2004) also used a probabilistic wave model coupled to a quasi one-line model in the long-term prediction of shoreline evolution. The use of probabilistic wave models is one method that avoids the need for exact chronologies and has been able to produce accurate morphologies.

Ruessink (2005a) suggests that one problem with conventional models is their inability to deal with uncertainty. This type of uncertainty could include inaccurate initial or driving conditions as discussed in the previous paragraphs. Many errors may be introduced into the model. A poor description of processes may introduce errors associated with the model structure. However, this is associated with current theoretical knowledge rather than the model development itself.

Forcing data and model input data, such as initial elevations and grain sizes, may contain measurement errors that propagate through the results. Traditional models are reliant on this data to develop the initial morphology over time. There is scope to develop a different modelling method that does not rely on this data so heavily, as was attempted by the inclusion of probabilistic rather than fixed wave data. A method that was not time-step based would also avoid some errors associated with input data, as the movement of sediment from an initial morphology would not occur with morphologies compared directly to one another to see which was closer to a state of equilibrium. This would reduce the potential for anomaly amplification.

A third major source of error is the uncertainty associated with the model parameters that govern the equations. Again, this is not so much controlled by the type of model used, but rather the calibration process and the available laboratory or field data with which to make comparisons. Model parameters are normally calibrated by trial and error, but a number of researchers have tried to implement an automated approach where a local-search gradient-based

algorithm or a global-search algorithm is utilised to find near optimal values for parameters (Ruessink, 2005b). Unfortunately due to the shape of the solution space, Ruessink (2005b) found that similar near optimal results were obtained with largely varying parameters so the success of the automated approach was limited. In this situation knowledge of the expected values is beneficial, in order to make an informed decision as to which parameter values are more realistic. In a similar way to Rinaldo et al. (1998), Ruessink (2005a) suggests that rather than a single optimal set of equation parameters, a range may exist due to their interdependence and insensitivity.

A method is needed that overcomes some of these conventional model problems. The research contained in this thesis aims to exploit entropy-based and self-organisation-based methods to this purpose.

There are three main types of entropy – thermodynamic, statistical mechanical (Boltzmann) and information (Shannon) entropy. Physical entropy incorporates both statistical and thermodynamic entropies (Fiorentino et al, 1993; Kapur and Kesavan, 1992). Information entropy is subjective and can be used to maximise the information available (Shannon, 1949). All three types of entropy have been used in the past either directly, or through analogies, to predict equilibrium landscapes (Sukhov, 1967; Zdenković and Scheidegger, 1989; Cao and Knight, 1996; 1998; Reggiani et al., 1998). However, the topic of this thesis deals with theories derived from thermodynamic entropy analogies, so past research in this area only will be concentrated on in the following Sections.

2.2 Use of Entropy-Based Equilibrium Modelling in River Morphology

The use of entropy-based methods to predict equilibrium morphologies was sparked by Leopold and Langbein (1962) over forty years ago. They used minimum work as a criterion based on entropy with which to predict the equilibrium longitudinal profiles formed by rivers, and they compared their predictions to field measurements. An example of longitudinal river profiles derived by entropy-based methods is shown in Figure 2.3.

Since Leopold and Langbein's pioneering efforts, many river morphologists have expanded on their principles, using "extrema hypotheses" such as minimum unit stream power, minimum energy expenditure and maximum sediment transport capacity to predict equilibrium river profiles and networks (Yang, 1971; 1976; Yang and Song, 1979; Yang et al., 1981; Bettess and White, 1987; Chang, 1988; Maritan et al., 1996; Deng and Singh, 1999; 2002; Huang et al., 2002; Huang et

al., 2004). In these hypotheses, the relationship between energy and entropy is exploited, where a system will tend towards a state of maximum entropy or minimum entropy production if the system is closed or open, respectively. The definitions of open and closed systems are given in the following Section, as well a description of thermodynamic entropy and the analogy alluded to by Leopold and Langbein (1962).

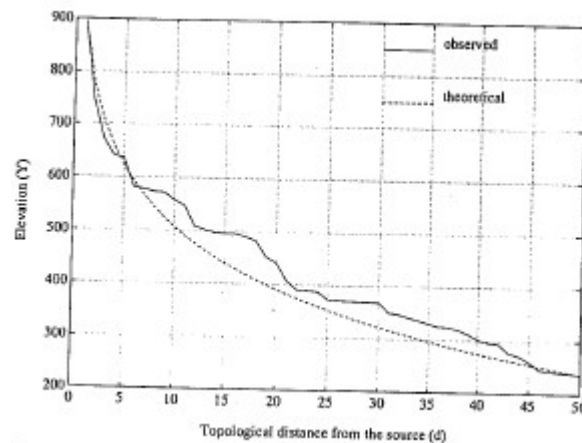


Figure 2.3 Typical longitudinal equilibrium river profile determined by using entropy-based principles (after Fiorentino and Claps, 1992).

2.2.1 Open, Closed and Isolated System Definitions and Entropy Behaviour

In order to understand the relevant research that has been undertaken in the past using entropy-based methods to model equilibrium morphologies, an understanding of the definitions of open, closed and isolated systems is required. It is also important to differentiate between the different behaviours of entropy in these systems.

A system can be defined as a group of elements that have certain attributes dependent on the attributes of other elements in the system (Scheidegger, 1988; 1992). For example, a coastal system would include the beach and water some distance offshore. The shape of the sand on the beach is dependent on the wave energy from the water that washes over it at high tide.

Systems can be defined as open, closed or isolated, depending on the interactions of energy and matter between the system and its surrounds. When considering entropy, and whether its production increases or decreases in a system, it is imperative to define the type of system as this determines what happens to the system's entropy as the system approaches equilibrium.

System Definitions

Open systems (see Figure 2.4) are defined as systems where energy and matter is exchanged between the environment surrounding the system and the system itself (Prigogine, 1967). Most systems in nature, including geomorphic and coastal systems, can be considered open (Scheidegger, 1988; 1992; Prigogine, 1967).

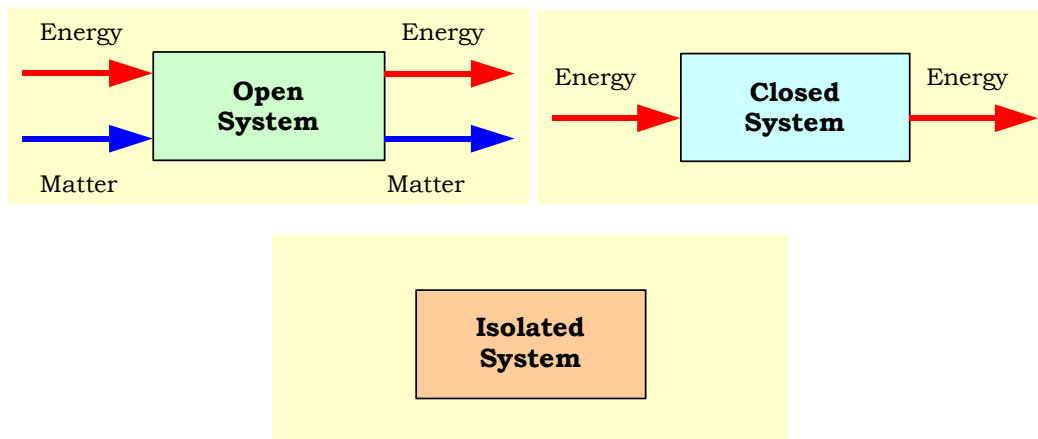


Figure 2.4 Definition of Open, Closed and Isolated Systems

Closed systems (see Figure 2.4) are a special form of open systems where there is no matter exchange between the system and its environment, but energy exchange may still occur (Prigogine, 1967).

Isolated systems (see Figure 2.4) are an even more specialised group of open systems, where there is neither energy nor matter exchanged between the system and its environment (Prigogine, 1967).

Entropy Behaviour in Each System Type

The entropy of closed and open systems is the summation of the system entropy (internal entropy) and the entropy of the surrounding environment (external entropy) (Prigogine, 1967). This means that if energy is input from the surrounds, the system may actually become more ordered, or if energy is lost from the system, the entropy of the surrounds may increase but not the entropy of the system.

In an open system the Prigogine Principle states that the rate of entropy production decreases to a minimum value, per unit mass of the system, with respect to external constraints (Yang, 1994). External constraints may be things such as underlying geology for example, as a hard rock platform will constrain the erosion of sand on a beach.

In an isolated system, entropy always increases, as no energy is lost from the system, so any energy expended increases the entropy of the system (Singh, 2000).

Entropy enables the consideration of both global and local factors, for instance the movement of energy and entropy between the system and its environment, as well as the energy dissipation internally within the system (Phillips, 2002).

Thermodynamic entropy is the state variable associated with the second law of thermodynamics. Its common form is shown in Eq. 2.1.

$$dS = \frac{dQ}{T} \quad (2.1)$$

Where dS is the change in entropy;

dQ is the change in thermal or heat energy; and

T is the temperature in kelvin.

This definition of thermodynamic entropy was utilised by Leopold and Langbein (1962), to define the entropy of a longitudinal river profile at equilibrium, as is discussed in the following Section.

2.2.2 Leopold and Langbein's Analogy

Leopold and Langbein (1962) first alluded to an analogy between the height of a landscape and the temperature of thermodynamic entropy as shown in Eq. 2.2, which allowed them to predict equilibrium longitudinal river geometries.

$$dS = \frac{dM}{H} \quad (2.2)$$

where dM is the change in mass; and

H is the height of the landscape.

Scheidegger (1964) later proved this analogy. However, he placed some restrictions upon the analogy's application in open systems. It must be assumed that any deviation from equilibrium is proportional to the force required to restore the system to equilibrium ("the regression of fluctuations is linear"). The "principle of microscopic reversibility" must also be assumed. This means that any small change either side of equilibrium is reversible (i.e. if a small mound is formed in a channel, it is possible for it to be eroded and equilibrium restored, conversely, if a small hole is made, it is possible for it to fill and equilibrium to be restored). The analogy is therefore valid for open systems, provided the landscape in question is observed from an overall perspective (such as the

formation of a lake), not a minute perspective (such as local processes including sedimentation in lakes).

Leopold and Langbein's Incorrect Use of Entropy Methods

The use of entropy hasn't always been successful. Throughout its history there have been misinterpretations and misuse of entropy due to incorrect system definitions, incorrect applicability of conditions in which analogies are valid and incorrect mathematical understanding.

Leopold and Langbein (1962) applied the principle of maximum entropy to a system that they defined as closed, but their definition of a system in which there was no exchange of matter or energy was actually the definition of an isolated system (according to the definition given by Prigogine, 1967). This same isolated system/closed system definition confusion was made by Chorley (1962), as was mentioned by Sherman (1996). Davy and Davies (1979) criticised Leopold and Langbein (1962) for the misuse of entropy purely on thermodynamic grounds, as their system was not isolated.

Scheidegger (1964) also criticised Leopold and Langbein's (1962) poor assumptions and definition of the analogy, but went on to prove the analogy and the valid assumptions that must be applied (as mentioned in earlier in this Section). Langbein (1964) used this work to rebut Kennedy et al's (1964) claim of mathematical mistakes in the initial 1962 paper.

Later Scheidegger (1988) agreed with Davy and Davies (1979) that the use of a thermodynamic analogy for river geometries is probably not valid for the case used by Leopold and Langbein (1962).

Scheidegger (1992) stipulated that the use of system theory could only be applied to exogenic or degradation processes, as these were quasi-random, hence statistical-mechanical entropy could be applied to them. Structural and tectonic landscapes are endogenic (rather than exogenic landscapes which are created by weathering processes) and therefore the theory does not apply, as they are deterministic in nature. Phillips (1994) suggested that the reason landscapes appear complex and random, may be due to chaos. He hypothesised that turbulence, which is chaotic, may transfer some of its chaos to the underlying sediment.

Following Leopold and Langbein's pioneering research, others have gone on to develop new theories, using similar ideas, but based on better defined theories and principles. These are discussed next.

2.2.3 Extrema Hypotheses and Their Use in Fluvial Systems

For many years, researchers have been trying to determine the equilibrium profiles of rivers. Based on the early entropy-based work of Leopold and Langbein (1962), but without some of their misconceptions, one common thread of research has looked at using extrema hypotheses to determine the profiles of rivers in dynamic equilibrium. Dynamic equilibrium is defined as when a system hovers around equilibrium, with minor fluctuations in either direction. Its actual equilibrium state can only be determined statically.

Extrema hypotheses is the name given to a collection of methods which enable dynamic equilibrium formations such as river networks or longitudinal stream profiles to be determined through the use of an optimisation routine. These hypotheses methods avoid the need for the time stepping used in process-based models, and hence some of its associated problems as discussed earlier in Section 2.1.1. The need for an optimisation routine arises from the fact that there are a number of unknowns or degrees of freedom present in a river system for example, and not enough equations to solve them. Another equation derived from entropy-based or empirical relationships must therefore be utilised. For example, in a river system there exist at least three degrees of freedom, namely depth, width and roughness, from which all other variables (such as slope) can be calculated. The equations of continuity and momentum are not adequate for use when a movable boundary such as a riverbed is involved, as there are more unknowns than equations (Yang, 1994). Therefore a third equation is needed to solve the unknowns, which is commonly achieved by the use of an extreme hypothesis.

Extrema hypotheses include optimisation methods such as maximum entropy (Leopold and Langbein, 1962), minimum unit stream power (Yang, 1971), minimum stream power (Chang, 1979), minimum Froude number (Yalin and Ferreira da Silva, 2000) and minimum rate of energy dissipation, which have been used to determine river networks by researchers such as Yang (1987) and Rodríguez-Iturbe et al. (1992).

Methods that use only the Newtonian laws of continuity and momentum are known as vectorial methods, while the use of energy and entropy-based principles such as those used in extrema hypotheses, where potential and kinetic energy are considered, are known as variational theories.

There is much debate on the relevance of extrema hypotheses. They are primarily empirically based, with the help of field or laboratory observations,

rather than theoretically based. There are exceptions to this however. Yang (1987) argued that the principle of minimum energy dissipation is indeed theoretically based, unlike the theories of maximum friction factor or maximum sediment transport for example. This is because it can be derived using variational theory, and its form can be equated to a vectorial approach in some cases. Areas where the principle of minimum energy dissipation has been used effectively in the past are therefore elaborated on in the following Section.

2.2.4 Minimum Energy Dissipation Rate

Minimum rate of energy dissipation is a general theory that has been used as a method for determining optimal river shapes and paths. It was defined by Yang and Song (1979) as the 'integral of unit stream power'. A river strives to minimise its energy dissipation rate, by adjusting its flow and boundary conditions such as velocity, turbulence, sediment transport, geometry, roughness, slope, the formation of riffle-pool systems and meanders, subject to constraints such as those imposed by geological factors, climatic factors and human constructions.

Minimum rate of energy dissipation can be applied to any system that is closed and dissipative, or to an open system that is converted to a closed system (Yang, 1994). A hydraulic system can be thought of as dissipative, as in this type of system, potential energy is converted to kinetic energy. Some of this kinetic energy is then converted to heat (or molecular) energy and lost across the system boundary.

Yang (1987) suggested that the minimum energy dissipation rate is theoretically based on variational principles, and unlike extrema hypotheses such as maximum friction factor or sediment transport capacity, it can be applied to situations other than those involving fluvial systems. In special cases it can even be shown as equivalent to the more widely accepted vectorial theories. This suggests that it can be applied to coastal morphological prediction. In the past it has been applied in the determination of stream geometry (Yang and Song, 1979; Yang et al., 1981;) and the recognition of optimal stream networks (Rodríguez-Iturbe et al., 1992). An example of an optimal stream network is shown in Figure 2.5.

The work of Yang laid the foundations for this theory, but its most widespread and applicable use has been in the field of optimal river network determination. The patterns formed by river networks are in some respects similar to the channels that form in a tidal-channel system (Cleveringa et al., 1997). Therefore,

knowledge gained in this area can be applied to the prediction of stable estuary morphologies. The next Section discusses past investigations of optimal river networks.

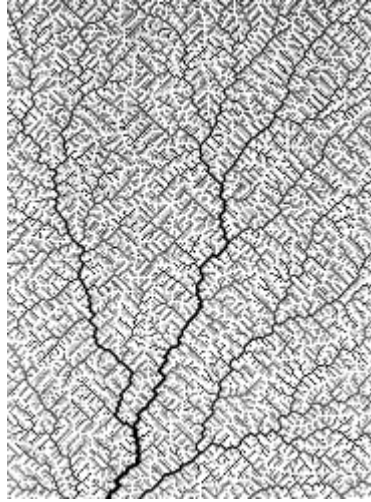


Figure 2.5 Optimal channel network (after Rinaldo, 1999)

Optimal River Networks and Energy Expenditure

Molnár and Ramírez (1998) used energy dissipation theory in the prediction of optimal channels and river networks. They minimised energy dissipation both locally and globally. Locally, the rate of energy dissipation per unit channel area was made as uniform as possible subject to constraints. Making energy as uniform as possible throughout the channel is similar to the methodology used by Leopold and Langbein (1962), Yang (1971) and Langbein (1963) in his examination of estuaries. Globally, the total rate of energy dissipation in the entire river network was minimised. Together, these two criteria work towards the formation of an optimal river network, one in dynamic equilibrium. Molnár and Ramírez (2002) found that their method was able to explain the formation of two different river systems in the field. Their work is similar to that of Rodríguez-Iturbe et al. (1992), who as well as the above-mentioned criteria also minimised the energy dissipation between two river links in order to determine optimal stream networks. Banavar et al. (1997) and Rinaldo (1999) have both shown that a longitudinal profile can be developed from a random starting configuration by applying these principles and accepting or rejecting perturbations. This research shows that this method is not as reliant on starting conditions and equilibrium river networks can be recognised directly without time-stepping.

These energy dissipation principles have been used in conjunction with a global search method, namely simulated annealing, in order to determine a near

optimal river network by Rinaldo et al. (1998). However, Rinaldo (1999), Rinaldo et al. (1998) and Banavar et al. (1997) all agree that a river system may not strive to form a unique optimal network, but is happy to reside in a number of similar ones that may be formed without having to increase energy expenditure temporarily in the process of reaching a more energy efficient network. This finding is important in the prediction of two-dimensional lagoon morphologies such as those analysed in this thesis. It suggests the predicted morphology may not be the end bed profile developed by the system, but that this profile may develop into a similar stable morphology close to the global one, but without the need to move to an interim state with greater energy dissipation. Although the morphology may be slightly different, the overall hydraulic characteristics of the system should be similar to the global state if the energy dissipation in the system is similar.

The global optimisation search routines employed in this thesis and described and discussed in Section 2.3 and Chapter Four, Section 4.2, are able to predict near optimal morphologies, as their search methods allow them to escape from local minima in the solution space. At equilibrium, a number of morphological configurations may give similar energy dissipation values, and the hydraulics of these configurations should also be similar. Therefore it is postulated that even if for example, the physical system does not reside in the exact global equilibrium morphology, the general configuration should be similar to that predicted using an entropy-based approach. Maritan et al. (1996) observed this when they predicted local minima at which optimal river networks occurred. They considered elevation difference and water flow in the determination of energy dissipation over river networks similar to those pictured in Figure 2.5.

Cleveringa et al. (1997) gave further insight into tidal-channel systems that are of interest to research involving estuary morphology predictions. They suggested that tidal-channel networks are an example of fractal landforms. Fractal landforms are landforms that have the same pattern independent of spatial scale. For instance, the pattern formed on a beach may be mistaken for a mountain range if a person is shown a picture of the two landforms without being given corresponding scales. Another example is the rill patterns due to runoff down a hillside that form similar patterns to river networks, but at a much finer scale. Feedback in this type of system occurs due to current and morphology interactions, while hydrodynamics constrain the system.

Fractal landforms are often associated with self-organising patterns as the same shape is formed repetitively. Rinaldo (1999) is in agreement with Cleveringa et

al. (1997) and hypothesised that channel networks form as a result of critical self-organisation (see Section 2.4 for a discussion on self-organisation).

Discussion so far has concentrated on research by river morphologists into the use of extrema hypotheses as this is the area where the majority of exploratory research has been undertaken. The following Section outlines a few cases where these ideas have been used in coastal modelling.

2.2.5 The Use of Other Entropy-Based Analyses in Coastal Environments

To the author's knowledge little work has been undertaken on applying the previously discussed entropy-based principles to coastal situations. This is an area where further research would be beneficial. The following paragraphs outline coastal research that has been undertaken in this area.

It has been shown by Friedrichs and Aubrey (1996) that uniform maximum velocity can be used to derive equilibrium profiles on tidal or wave dominated beaches and bays, in the case where a constant drag coefficient is assumed and therefore maximum velocity is equivalent to maximum shear stress. Their work is comparable to observations made by river morphologists and was able to predict similar equilibrium profiles to those observed in the field.

Wright et al. (1973) used Leopold and Langbein's observations to analyse two different deltas in Western Australia and determine whether they were at equilibrium. They were able to extend their reasoning to analyse the development of a number of characteristic deltas around the world. An example of the planform river deltas they analysed is shown in Figure 2.6.

Wright et al. (1973) considered the formation of equilibrium tidal channels that satisfied uniform work distribution, minimum work on the channel boundaries and hydrodynamic continuity. They calculated these values using planform measurements, for the shapes of a number of river deltas and determined whether they were at equilibrium according to their current dimensions. Minimum work on channel boundaries was similarly used by Molnár and Ramírez' (2002) to determine optimal river channels. Hydrodynamic continuity in the system can be considered as a constraint, similar to those placed on stream networks formed by extrema hypotheses.

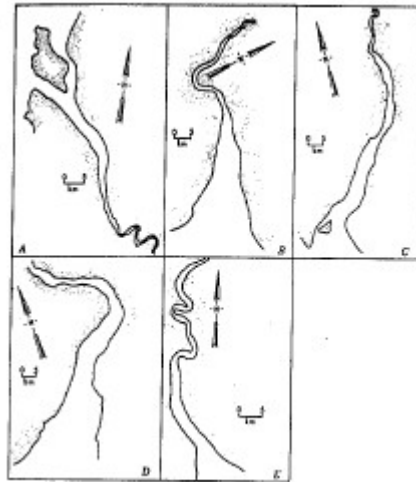


Figure 2.6 An example of five river delta channels analysed by Wright et al. (after Wright et al., 1973)

The work of Wright et al. (1973), suggests that theories used in river equilibrium predictions apply to tidally influenced inlets, but their work considered only the planform of the estuaries. One possible reason that this work was not expanded is the lack of computer power and suitable global optimisation methods during the time period that Wright et al. undertook their research. This seems to be a common trend in this area of research; there are lots of theoretical examples but little application. The topic of this thesis is to expand the use of these entropy-based equilibrium principles to predict morphologies such as those associated with tidal lagoons, and hence hydrodynamic properties that a system evolves towards when a dynamic equilibrium is reached.

The key to utilising these entropy-based modelling methods is the development of an objective function using principles such as minimum energy dissipation. This objective function must then be minimised using a suitable optimisation routine. Two different global optimisation routines are compared and contrasted in the following Section.

2.3 Optimisation: A Comparison of Genetic Algorithms and Simulated Annealing

There are many different types of global optimisation methods available, capable of handling complex objective functions, all with positive and negative points associated with them. All need to be tailored to the problem to some extent, and their effectiveness is limited by the user's ability to manipulate them and choose the correct empirical settings. Genetic algorithms (GAs) and simulated annealing (SA) are two methods that are based on natural processes and have been applied effectively to a variety of problems where objective functions can be defined

(Mahfoud and Goldberg, 1995). This Section will concentrate on the discussion of these two methods.

It has been suggested that GAs and SA are capable of handling optimisation that involves a large number of decision variables (Athias et al., 2000). This is an important attribute, as when applied to the case studies utilised in this thesis, the values of a large number of decision variables must be determined. GAs are based on Darwin's "survival of the fittest" ideals while SA is based on the annealing of a metal (Kirkpatrick et al., 1983; Goldberg, 1989). The methods involved with each are outlined in detail in Chapter Four, Section 4.2. GAs have been found to be more robust than SA as SA is highly dependent on empirical input values for things such as starting temperature and cooling rate which control how fast the SA descends towards finding an optimal solution, both its efficiency and accuracy. These empirical values must be changed on a trial-and-error basis, in order to find the best combination for each individual problem, as was observed by both Wang and Zheng (1998) and Thyer et al. (1999).

Cunha and Sousa (2001) applied a SA algorithm to a hydraulic infrastructure problem and found that it outperformed a GA used by Dandy et al. (1996). SA has been found to outperform binary GAs (BGAs) as it eliminates the poor precision caused by the discretisation of decision variable values. BGAs use a string of zeros and ones to represent each decision variable. This allows simplified genetic modifications such as crossover and mutation to occur, but reduces the accuracy of the answer, as it is not continuous as in a real coded GA. More bits (zeros or ones) are required in the string to increase the accuracy of each decision variable. A longer string increases the computation time required. A number of authors mentioned poor precision as the cause for the failure of a BGA to perform as well as SA (eg Lin and Yeh, 2005; Wang and Zheng, 1998; Ingber and Rosen, 1992).

Very fast simulated reannealing is more likely to find a global optimum point than a BGA, it has also been found to converge faster. However, it is less efficient than a BGA as it requires a larger number of function calls, according to Ingber and Rosen (1992).

In other cases, BGAs have been found to outperform SA (Athias et al., 2000). When compared in the deduction of eight oceanic particle cycling rate constants, the BGA found the global minimum in fewer iterations. The GA was also more robust, being less dependent on starting values due to its population approach. It considers many different combinations of decision variables, all over the solution space, rather than a single combination as is considered in SA.

SA is better at fine-tuning, while GAs are good at finding the general area of a global minimum (Franconi and Jennison, 1997). This suggests that a combination of the two would produce a better search mechanism.

Soh and Dong (2001) used an interesting hybrid of GAs and SA, where SA was performed on the loser population member after tournament selection, to increase its fitness. They did not use crossover in their GA, only tournament selection and mutation. Mutation always occurred, but the type of mutation varied between uniform and random. The size of the mutation diminished after every 30 generations, which allowed the members to move closer to the global minimum. They also used mutation to create a new population member when infeasible members evolved. A description of these genetic processes is given in Chapter Four, Section 4.2.2.

Wong (2001) developed a different hybrid model, which utilised the Metropolis Criterion from SA to determine whether crossover or mutation in the GA module was accepted or rejected. This hybrid method was found to outperform a straight GA or SA module for the scheduling of multiple hydrothermal plants. A description of SA and the Metropolis Criterion definition is given in Chapter Four, Section 4.2.5.

Davidson et al. (2000) used SA to refine population members that had been roughly optimised by a GA. Their method was found to be a vast improvement on current modified maximum likelihood methods. After five generations, population members with a high fitness were subjected to a modified SA module. Perturbations were performed on each population member, where a decision variable was altered slightly. If the fitness was increased, perturbations continued. If the fitness was decreased, the change was rejected and a new change tried. If five rejections occurred, the SA ended for that population member and the GA continued.

Other hybrid methods have been devised which utilise an SA framework, where multiple SA algorithms are run on different population members simultaneously. At each temperature bracket, crossover and/or mutation are performed on the members devised at that temperature and the GA modifications are accepted or rejected based on a temperature criterion (Shieh and Peralta, 2005; Franconi and Jennison, 1997; Mahfoud and Goldberg, 1995). These hybrid methods were found to outperform comparison BGA and grey-coded GA modules applied to the same problem.

Franconi and Jennison (1997) applied a BGA and SA along with a hybrid SA incorporating crossover to statistical image reconstruction, which involved the optimisation of a problem with a large number of decision variables. This problem resulted in either 256 or 4096 decision variables being optimised for, depending on the size of the image. They found that with the larger of the two decision variable problems, the GA began to stagnate after 100 generations, as the probability of a GA finding the exact values of a very long string of decision variables was small, especially when elitist selection was not utilised and the best member from each generation was not brought forward unchanged to the subsequent generation. Jennison and Sheehan (1995) also stressed the importance of elitist selection. The SA worked better in the larger decision variable example of the Franconi and Jennison study, as it only changed one decision variable at a time. The combination of the two methods outperformed both the individual methods. Further research would be beneficial in this area, to determine a suitable global optimisation method, or hybrid method to optimise problems with a very large number of decision variables.

2.3.1 The Use of GAs and SA in Morphological Areas

SA and GA optimisation techniques have only been used to a small extent in the past in coastal related problems. In instances where they have been used, it has mainly been in the determination of parameter values without having to calibrate these values through trial-and-error. For example Medina (2001) used SA to separate incident and reflected waves in a wave flume experiment involving a breakwater and determine 17 parameter values.

Recently, Kizhisseri et al. (2005) used genetic programming to aid in the prediction of parameters associated with sediment transport modelling. In a similar way, Knaapen and Hulscher (2002) used a standard BGA to determine parameters required to model the regeneration of sandwaves after dredging. The objective function minimised the error between model predictions and field measurements. A similar method was also utilised to determine the parameters involved in the prediction of alternate bar movement in rivers and channels using a BGA (Knaapen and Hulscher, 2003).

Ruessink (2005b) also used optimisation to predict three parameters required in an alongshore current model and a cross-shore profile evolution model. The optimisation algorithm was highly successful in the current model parameter prediction, when compared to synthetically generated data, but not so successful in the evolution model due to the interdependence of the parameters. Ruessink

used a combined RGA and downhill simplex algorithm to first find the general vicinity of the global minimum and then refine it using a local search technique.

Davidson et al. (2000) used a modified GA that included SA to determine frequency dependent reflection coefficients, used in determining reflection from a sea wall or reef type breakwater. Bennett and Chua (1994) use an SA to determine flow in an open-ocean. They used it with an inverse modelling method, which makes use of good data in the inner area of the model and ignores data from poorly defined boundaries. It worked by the minimisation of the error between the field data and predicted model data (Copeland and Bayne, 1998). The common trend with the use of global optimisation routines in coastal modelling is their use to calibrate parameters rather than predict morphologies directly, which is the gap that this thesis attempts to bridge.

Simulated annealing was also used by Rinaldo et al. (1998) to determine the river network pattern that minimised the rate of energy dissipation (see Section 2.2.4 for a definition and discussion on the extreme hypothesis of minimum energy dissipation rate). This is the only example known to the author of the use of these global optimisation techniques in the determination of minimum or maximum objective function values used to determine equilibrium or stable patterns based on entropy derived methods. Therefore, the use of these methods in the work presented in this thesis is an improvement over current random walk or trial-and-error based methods.

2.4 Self-organisation: Its Use in River and Coastal Modelling

In contrast to the use of entropy-based minimisation objective functions, self-organisation-based models are another type of non-traditional method that have been used to model medium- and long-term equilibrium morphologies as well as determine major processes that control landscape development in exploratory type models (Luo, 2001; Murray and Paola, 1994). Self-organisation is a process where a combination of positive and negative feedback allows a system to self-organise itself into a stable or equilibrium state (Houser and Greenwood, 2005a, 2005b). Positive feedback is defined as a system reinforcing itself, where an initial irregularity such as a small hole or mound, influences the flow around it, and grows in size, with deposition areas forming around a mound and erosion areas forming around a hole. Negative feedback on the other hand, might occur where the maximum angle of repose of the sediment limits the depth of a hole or height of a mound. Feedback is very important in long-term modelling (van Leeuwen et al, 2003).

In a self-organising system, the system organises itself at a local level, with global patterns emerging from local interactions. Self-organisation is often modelled using a cellular automata type of model, where an area is divided into small cells and each cell interacts locally with its neighbour cells, according to imposed rules. Through positive and negative feedback associated with local cell interaction, where steady state conditions exist, a global stable shape may result. The resultant stable shape can be similar to the morphology determined by an entropy-based optimisation method, such as those in the literature discussed in Section 2.2. Hergarten and Neugebauer (2001) observed this when they applied a self-organisation based model to the formation of drainage networks and obtained similar formations to those derived by minimum energy expenditure methods. Cellular automata models generally include some sort of time-step mechanism, however, it may be abstract in that a growth rate is obtained which needs to be calibrated. Cellular models represent a potential method able to overcome some of the conventional models problems discussed in Section 2.1.1 (Nicholas, 2005).

Systems that are nonlinear most commonly form self-organised systems, particularly when the system is dissipative and processes involved are irreversible (Baas, 2002). These types of systems are common in nature (Tamburro, 1992). Self-organising systems are complex and pattern formation may lead to maximum entropy or minimum entropy production if the system is closed or open respectively. This suggests that self-organisation has its roots in entropy-based work (Baas, 2002). It has been observed in some chemical processes, that particles may self-organise and clump together, decreasing entropy so that elsewhere particles may become more random and increase entropy (Weiss, 1998).

Self-organisation has been recognised in diverse areas such as fish school formation (Stöcker, 1999), forest evolution (Soares-Filho, et al., 2002; Sprott et al., 2002) and Maya village layouts (Brown and Witschey, 2003). The literature discussed in this Section however, will concentrate on its application to geomorphic, hydraulic and coastal situations. The remainder of this Section discusses in detail self-organisation methodologies and the past applications of these ideals in cellular automata models.

Self-organised environments are generally modelled using cellular automata models. They are able to predict equilibrium morphologies without being dependent on starting values (Bolliger et al., 2003). In general, models start with randomly chosen coordinates, to which a number of simple rules are applied. An example of a simple rule used in fluvial landscape development is that if a

raindrop falls on a certain point, it may move north, south, east or west, carrying a certain amount of sediment with it (Favis-Mortlock, 1998; Crave and Davy, 2001; de Boer, 2001; Luo, 2001). The amount of sediment that moves is dependent on the slope of the adjacent cells, the amount of water already pooled on the cell and the elevation of the cell. The baseline of the system may be lowered when sediment exits the system, to mimic an open system rather than a closed one (de Boer, 2001). The cellular automata model does not represent how a real landscape forms; rather the pattern that is produced represents the large-scale morphological patterns that the landscape may exist stably at, with the rules representing the important physical phenomena that control the underlying system organisation. It is the end morphology that is of interest, not the steps in between (Favis-Mortlock, 1998; de Boer, 2001).

Self-organisation methodologies have been used to model a variety of different morphological systems, varying from the one-dimensional repetitive rhythmic patterns of aeolian sand dunes (Anderson and Bunas, 1993; Miao et al., 2001) to the three-dimensional singular pattern of a fluvial landscape (de Boer, 2001). As was discussed in earlier Sections of this Chapter, cellular automata models are an alternative form of modelling complex environments, which have been used in place of medium- and long-term landscape evolution models such as the SIBERIA erosion model (Hancock and Willgoose, 2002; Hancock et al., 2003; Willgoose, 2005). The following few paragraphs explain briefly the types of areas self-organisation has been used to model in the past and gaps and expansions that the research in this thesis begins to address.

Self-organisation based methods have been applied to explain a myriad coastal formations including beach cusps (Werner and Fink, 1993), large-scale coastline features such as capes and cusped forelands (Ashton et al., 2001), nearshore crescentic and transverse sandbars (Caballeria et al., 2002) and sorted sediment patterns on shallow continental shelves (Murray and Thieler, 2004). For example, Werner and Fink (1993) were able to apply simple sediment transport and hydrodynamic interactions to formulate beach cusps. This work was expanded by Coco et al. (2001), who showed that swash excursions could be used as a driving force in the formation of beach cusps, with water particles eroding and depositing sand based on a water particle carrying capacity. This carrying capacity was related to the water particle's initially prescribed velocity and the morphology of the beach the particle passed over. They proposed that the self-organised patterns might actually be the cause of standing edge waves, rather than because of them. There is not enough field evidence at present to determine whether this is the case or whether beach cusps form due to the

presence of edge waves. Coco et al. (2004) later went on to compare their model to field results and include the effects of tides and infiltration.

Caballeria et al. (2002) applied self-organisation methodologies to the modelling of nearshore crescentic and transverse sandbars formation. This differs from Coco et al.'s (2001) beach cusp prediction model as it used sediment transport, and current and wave hydrodynamics models in the nearshore region of the coastline, rather than the swash section of the beach as was considered in beach cusp formation. Caballeria et al.'s model was able to show that self-organisation does indeed have a role to play in the formation of nearshore sandbars.

Cellular automata models have also been applied in a number of geomorphology areas. Miao et al. (2001) simulated the formation of aeolian sand ripples and dunes by applying local transport rules governing saltation in a similar way to Anderson and Bunas (1993), but with the additional inclusion of slide due to angle of repose breaches. These rules created a mechanism for providing positive and negative feedback. They used wind direction and magnitude as a driving force. Kocurek and Ewing (2005) found that if the wind direction was altered, the dunes reoriented first at the crests, but this reorientation was able to propagate through the entire dune. Baas (2002) built a similar model to that of Werner and Fink (1993) and Miao et al. (2001) but added a rule governing the effect of vegetation on sand dunes. A value of vegetation cover was prescribed which controlled the amount of sand that could be eroded from any considered grid point. This was able to predict a better resultant dune pattern as it included vegetation patterns such as blowouts where vegetation was sparse. Pannell et al. (2002), in contrast to Miao et al. (2001) derived sand ripples under water through a self-organisation process. They considered the energy of both the flow and grain elevation along with an angle of repose avalanching rule, to determine how each grain moved.

Favis-Mortlock (1998) was able to apply rules pertaining to the initiation and development of small-scale rills to predict the large-scale rill pattern that evolved on a hillslope. Hergarten and Neugebauer (2001) used self-organisation to form drainage networks similar to those formed using minimum energy expenditure principles by Rinaldo et al. (1998). Discussions on minimum energy expenditure can be found in Section 2.2.4.

In Murray and Paola's (1994) braided river cellular automata model, water enters upper cells and flow direction is determined by slope, while sediment transport is moved based on the Exner mass-balance equation. The addition of vegetation rules to the model was able to produce a channel that better resembled those

found in nature (Murray and Paola, 2003). A further modification of the use of water slope rather than bed slope improved the model to give more realistic results (Doeschl-Wilson and Ashmore, 2005). Modifying the grid size and transport laws also improved the predicted morphologies. Coulthard and Macklin (2003) developed a similar model, which they used to analyse contaminated sediment movement in a hydrodynamic environment. This contaminated sediment model also considered water runoff that formed dendritic patterns over a vast area, with sediment moved in conjunction with the water.

De Boer (2001) was able to apply local erosion and deposition rules to runoff from rainfall events in order to predict the large-scale fluvial landscape that evolved from a randomly formed initial landscape, in a similar way to Luo (2001) and Crave and Davy (2001). These differ from the cusp and ripple examples, as an overall pattern is formed rather than a repetitive rhythmic pattern. The final landscape was similar regardless of the initial random landscape, which is a trait common to self-organised systems (Bolliger et al., 2003). An improvement to the above mentioned models was the addition of a sweeping mechanism in the model, allowing water to travel in multi-directions by applying the rules from all four model boundaries rather than the uphill boundary only (Coulthard et al., 2002). This inclusion allowed for the development of an upland river basin and alluvial fan. Sun et al. (2002) developed a model able to predict the morphology of a similar type of landscape, but used a hybrid model that included the discretisation of cellular automata models, but also real sized physical processes, similar to the process-based models discussed in Section 2.1.

In a similar way to the application of cellular automata models to landscape morphology, Fiorentino and Claps (1992) minimised the amount of energy expended when runoff occurred in the network and used field data to validate their model. This method shows a link between the research into the use of cellular automata models and those involving extrema hypotheses as discussed in Section 2.2.4.

A study by Jiménez-Hornero et al. (2003) is one of the few uses of cellular automata models where the self-organisation of sediment around solid structures has been examined. Jiménez-Hornero and colleagues examined the scour pattern that developed around numerous obstacles due to runoff using a cellular automata model for the sediment movement and a BGK model for water transport. A BGK model treats water movement using fictitious particles instead of a standard computational fluid dynamics approach (Dupuis and Chopard, 2002). Similarly, Dupuis and Chopard (2002) used a cellular automata model to predict the resultant scour pattern under a submarine pipeline.

The results of cellular automata models help to alleviate some of the possible problems with process-based models such as poor inclusion of nonlinearity and amplification of errors due to time stepping. This type of modelling does not involve time stepping as such, but relies on a number of rules, which when applied over a number of iterations allow the final stable pattern to be deduced.

As can be seen from a review of the literature, the use of self-organisation-based cellular automata models is still in its infancy. In general, they are used as exploratory models, to determine which processes impart a large governing effect on the formation of different landscapes. However, a small amount of work has been undertaken, to compare the model results obtained to field or laboratory results, at least qualitatively (Favis-Mortlock, 1998; Crisci et al., 1999; Jiménez-Hornero et al., 2003). There is a need for further field and laboratory comparisons, including quantitative studies comparing traditional models to cellular automata model results.

There is much scope to expand this type of modelling to other areas where stable patterns form in the presence of structures, such as tombolos and salients behind breakwaters, and the complex morphologies of estuaries. Most of the models deal with purely erodible material, in particular the formation of rhythmic, repetitive patterns, without the inclusion of solid structures that may impart an influence on the self-organisation of the system around them. With the exception of the studies by Jiménez-Hornero et al. (2003) and Dupuis and Chopard (2002), little work has been undertaken in this area to the author's knowledge.

2.5 The Research Gap

In order to manage and design structures such as breakwaters, jetties, bridges and lagoons, it is important to be able to produce models of the different morphologies that may result under different conditions in the medium-term as well as the short term. Currently this is usually done using process-based time-stepping models that have a number of possible limitations including the amplification of small anomalies over the duration of the run and long computation times. These possible limitations are discussed in detail in Section 2.1.1. There is a need to develop different modelling methods that are able to overcome some of these possible limitations. In river morphodynamics researchers have utilised entropy-based methods to determine large-scale one-dimensional and planform morphologies of rivers and fluvial landscapes. This thesis elaborates on these methods, expanding them to be applicable to coastal situations such as those associated with a sandy lagoon, where the resolution of

the morphology is of a much finer scale and of greater dimension. Most importantly the models developed in this thesis search for equilibrium morphologies directly, without the need to reach them through time stepping and arriving at a prediction when sediment is no longer being transported as in conventional methods.

Much of the work published on entropy-based principles has dealt with the theory involved. The current research applies this theory to an actual situation and compares the results to laboratory data. To do this, global optimisation routines are utilised, which are modified from their usual forms so as to be able to deal with a large number of decision variables.

Self-organisation-based methods, using cellular automata models, are an alternative to process-based models that have been used to model medium- and long-term equilibrium morphologies of rhythmic repetitive features such as beach cusps and sand dunes. Little work has been attempted applying these to situations where solid structures interacted and a single self-organised stable landscape resulted. This area of research is covered in this thesis as well as the use of quantitative analysis between a laboratory study and traditional modelling methods.

The following Chapters address some of the gaps in the literature, adapting entropy-based and self-organisation-based methods to the prediction of equilibrium morphologies associated with constrictions, obstructions, lagoons and breakwaters.

3 Self-Organisation-Based Method and its Application to River Channels and Lagoons

One aim of this thesis was to develop a type of model capable of predicting equilibrium morphologies that was an alternative to traditional process-based models. The ability to predict equilibrium morphologies is necessary in order to design and manage coastal and river systems that involve engineering structures such as breakwaters or bridge piers. One non-traditional modelling method that has been used previously to model coastal and river environments is based on self-organisation.

Self-organisation refers to the phenomenon, where positive and negative feedback influence a system, and may result in the formation of a stable morphology. A cellular automata model is a form of modelling that allows for this feedback to occur. Local rules are applied on a cell-by-cell basis, resulting in the formation of a global, stable morphological pattern. In the past, cellular automata models have been applied in diverse areas such as fish school formations or Mayan village layouts (Stöcker, 1999; Brown and Witschey, 2003). They have been particularly useful in the exploration of factors that influence the formation of beach cusps or longshore bars (Caballeria et al., 2002; Coco et al., 2004). This Chapter outlines the development of a self-organisation-based, cellular automata model.

The model discussed in this Chapter is similar in some respects to models developed by researchers including Werner and Fink (1993) and Coco et al. (2004) which look at modelling rhythmic, repetitive beach cusps. It is similar in that it uses a cellular automata model framework and applies a number of similar sediment movement rules. It differs from these however as it investigates the movement of sediment around fixed structures, including an obstruction or constriction in a channel or the lagoon surrounding a river mouth (see Figure 3.1). It uses water velocities as a driving forcing for sediment self-organisation, as well as physically based avalanching.

The method used is based around simple rules, applied locally to produce a global stable pattern. The rules are applied in a cellular automata type model and are based around critical velocity and angle of repose. Small increments of sediment are moved locally from cell to cell based on these rules, and the subsequent flow field is determined by a hydrodynamic solver. The model is efficient to run and is able to predict similar shapes and hydraulic performance

to those measured in the laboratory, and those obtained using a more conventional method. It is a useful extension of previous research as it has the potential to benefit areas of coastal research such as the prediction of equilibrium formations behind a detached breakwater or the scour that develops around bridge piers in a river environment. It could also be used to model more complex environments where errors have a tendency to be amplified, or traditional models that have uneconomical computational times.

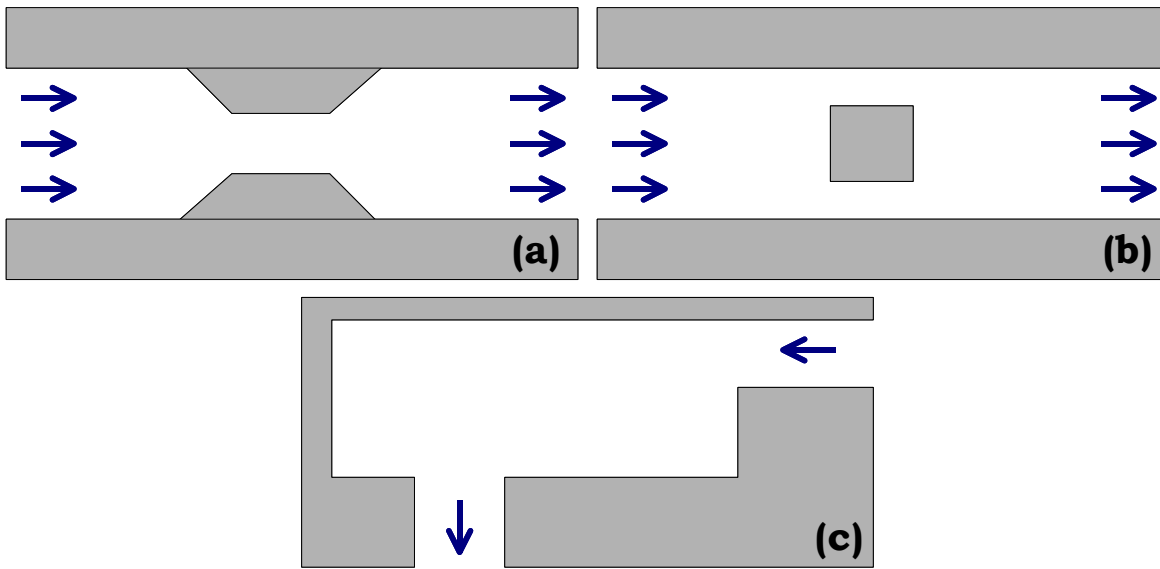


Figure 3.1 Description of modelled case studies (a) a channel constriction, (b) a channel obstruction and (c) a unidirectional lagoon.

The developed model represents a novel way of modelling coastal systems involving structures. It is an alternative to conventional time-stepping models, as it uses an iteration step as the model progresses, without the reliance on sediment transport formulae often required in traditional process-based models. Instead it requires an accurate formulation for the initiation of sediment transport rule. It also requires a clear-water scour system, where an equilibrium morphology is reached when sediment is no longer transported through the system. Throughout this Chapter, comparisons are made between the cellular automata model, a traditional model that uses the same hydrodynamic model as the cellular automata model, and a number of laboratory studies.

3.1 Method Description

This Section details the method developed, the workings of the cellular automata model and the rules applied in the determination of stable morphologies

associated with the three case studies pictured in Figure 3.1. A copy of the code for the developed model can be found in Appendix A.

There are two main components to the model that allow for the sediment to self-organise itself. The first is the cellular automata part, where rules are applied to individual cells, inducing local interactions that bring about global self-organised patterns. The second part involves the application of a Navier-Stokes flow model, where flow patterns are calculated which act as the driving force for the model and allow the rules to be applied to each cell based on flow predictions. The 2DH Navier-Stokes flow solver uses a staggered grid finite difference model to determine the flow field. Details of the hydrodynamic model can be found in Section 3.3.

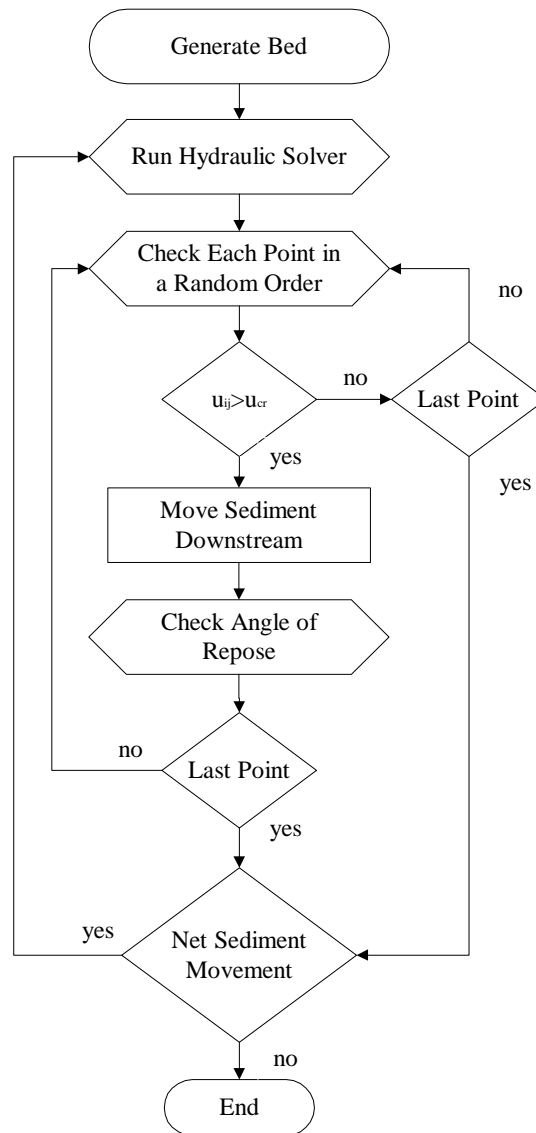


Figure 3.2 General description of model methodology.

The rules are applied to each cell individually in a random order at each iteration step. This means that one direction is not favoured over another. After each cell in the model has been assessed, new flow patterns are calculated for the resultant morphology. This means that the flow field is constantly adapting to the morphology and helps to allow for positive and negative feedback between the water and sediment. The iteration process is stopped when the model has been deemed to reach an equilibrium morphology. The equilibrium morphology is determined when sediment is no longer moved according to the rules. Initially a flat bed or bed with small random undulations is established and the rules are then applied. A general outline of the method is given in the flowchart in Figure 3.2.

The developed models incorporate two rules to determine sediment distribution. Firstly, if the velocity of a cell is greater than the threshold velocity, sediment is moved to adjacent cells in proportion to the velocity vectors leaving the cell in question. The cellular automata model uses a Von Neumann neighbourhood, so sediment cannot move in a diagonal direction (Wolfram, 2002). A description of this neighbourhood type can be seen in Figure 3.3.

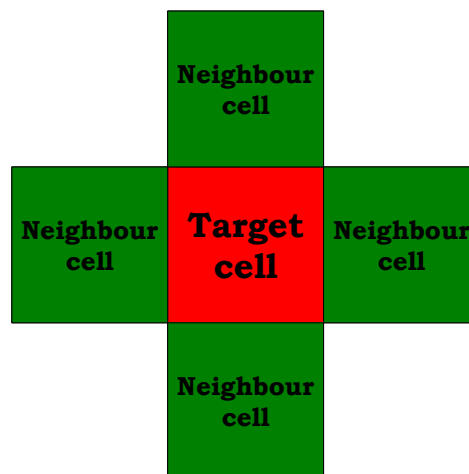


Figure 3.3 Von Neumann neighbourhood.

The amount of sediment distributed between adjacent cells varies depending on a sediment increment chosen. In the set of scenarios analysed in this research, increments of between 10mm and 0.5mm in depth were analysed, with a sediment increment of 1mm being utilised for the majority of numerical runs as this reduced computational time but still gave an accurate resultant morphology (see Section 3.8.2 for a discussion on model sensitivities). The threshold velocity value is calculated using van Rijn's (1984) equation, given in Eq. (3.1).

$$\bar{u}_{cr} = 0.19(d_{50})^{0.1} \log_{10} \left(\frac{4h}{d_{90}} \right) \quad \text{for } 100 \leq d_{50} \leq 500 \mu\text{m} \quad (3.1)$$

where \bar{u}_{cr} is the critical mean flow velocity in metres per second;

h is the water depth in metres; and

d_{50} and d_{90} are the 50th and 90th percentile of sediment size (percent passing) expressed in metres.

The second rule represents negative feedback as it keeps the system in check and prevents areas of deposition and erosion growing indefinitely. If the slope between two adjacent cells is greater than the angle of repose, an avalanche occurs, reducing the slope to a random slope of a value between 50 and 100 percent the angle of repose. This range was found to produce the most realistic depositional shapes when compared to laboratory results. This is discussed in sensitivity analyses documented in Sections 3.4 and 3.8. The randomness is incorporated to try to mimic nature, where an avalanche will rarely bring a slope back to exactly the angle of repose (Blom, 2003). The sediment that avalanches is distributed down slope of where the avalanche occurs, with the potential for this redistribution to initiate further avalanches. The avalanche rule is very important in the small-scale laboratory situations, as it prevents unrealistically steep slopes from developing. In the large-scale lagoon example the coarseness of the grid and the shallowness of the water mean that there is little opportunity for a difference in angle between cells to be greater than the angle of repose. A coarse grid was used to reduce computational time, but if the grid size was reduced, the angle of repose rule would be equally important in the lagoon case study.

The method described above differs from traditional models as time-stepping is applied in an abstract way. In contrast, the model moves in sediment increment steps until a stable morphology results. As the size of the sediment increment moved in each iteration is kept constant, the time taken to move each increment may change, so the model works using an increment step rather than a conventional time step.

Stöcker (1999) put forward a number of criteria that should be satisfied by any cellular automata model. The model discussed in this Chapter meets these criteria. Firstly, the model must be of a grid structure (cellular space), which is commonly rectangular. This condition is met in the developed model, as a square grid is used. Secondly, each grid site should be assigned a number of finite values (state space). This condition is met as each grid point can have a certain sand elevation. Thirdly, the neighbourhood criterion must be met where

the evolution of each grid cell is dependent on the application of local laws between it and its nearest neighbours. This condition is met as the local laws of sediment transport if velocity is above critical, and adhesion to a maximum angle of repose are both applied on a cellular basis, between neighbouring cells. Fourthly, the system must evolve in discrete steps (state evolution). The developed model consists of discrete iteration steps. Finally, boundary conditions must be considered. These are considered differently depending on the case study.

According to Wolfram (1984), the cellular automata models developed in this research are of class one type, “limit points”. In this class, different starting conditions move to similar end conditions after a finite number of iterations. This is in agreement with other literature that suggests a common trait of cellular automata models is their insensitivity to starting conditions (Bolliger et al., 2003).

3.2 Channel Constriction Case Study: Laboratory Method and Results

In the first instance, a laboratory case-study was undertaken that consisted of a erodible bed channel with unidirectional flow through a constriction placed in the centre of the channel. Erosion occurred in the throat of the constriction with deposition downstream. A description of the case study is shown in Figure 3.4. This Section gives a detailed description of a number of laboratory experiments undertaken.

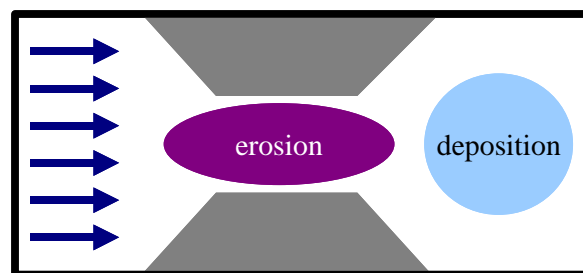


Figure 3.4 Constriction case study description.

A number of laboratory experiments were undertaken in a flume approximately 10m long, and 0.914m wide, that contained a constriction in its centre. A diagram of the experimental set-up can be seen in Figure 3.5.

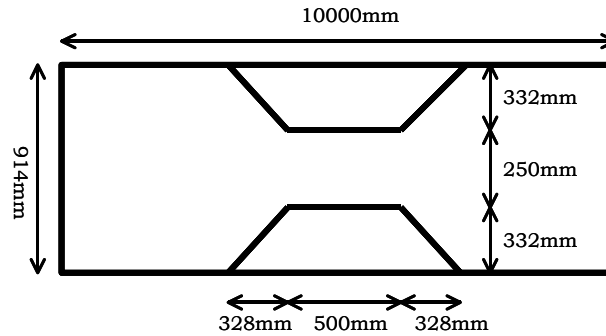


Figure 3.5 Constriction laboratory set-up.

A wooden constriction was placed in the centre of the flume and attached with silicon to the flume sides. The width of flow reduced to 0.250m through the constriction. The length of the constriction included a straight tapering section 0.328m long, followed by a uniform section 0.500m long and a second taper also 0.328m long.

Sand was placed throughout the flume to a depth of 0.3 m and sand traps were secured at either end to prevent loss of sand. These traps contained a number of small holes to allow water to drain after the experiment, but were temporarily blocked during the experiment to minimise flow through the sand substrate.

The bed was first flattened and prepared with the use of a spirit level and levelling block to create a negligible bed slope in both the longitudinal and transverse directions. Water was then slowly allowed to enter the flume during a one to two hour period. The flume was filled to an approximate depth of 0.2 metres without the disturbance and remoulding of the flat sand bed. At this point, water began to spill over the weir at the end of the flume. A flow rate and average depth were then chosen so that the constriction area was subject to clear water scour. (See Table 3.1 for the exact flow conditions of each experiment.)

Table 3.1 Flow conditions used for each of the six experiments.

Trial Number	Flow Rate ($\text{m}^3 \text{s}^{-1}$)	Flow Depth (m)
One	0.0231	0.272
Two	0.0204	0.268
Three	0.0267	0.276
Four	0.0231	0.270
Five	0.0219	0.266
Six	0.0226	0.266

Water circulated through the flume until the bed reached an equilibrium profile and the sand movement became negligible throughout the flume (typically one to two hours, with final morphologies measured after six to eight hours).

3.2.1 Flow and Depth Measurements

The initial centreline water depths upstream and downstream of the constriction were measured in each experiment using a pointer gauge. For each experiment a volumetric tank with a cross-sectional surface area of 2.178m², was used to measure flow rate. The time taken for water entering the tank to raise the tank depth from half a metre to one and a half metres was measured. This was repeated five times and the average flow rate was calculated.

3.2.2 Velocity Measurements

During selected experiments, velocity and depth to bottom measurements were taken periodically in the erosion areas using an Acoustic Doppler velocity meter (ADV). Once a quasi-equilibrium state was reached, a number of cross-sectional velocity profiles were also measured using the ADV.

For these experiments, the ADV probe was positioned in the throat of the constriction. It was placed close to the incoming flow for each of the experiments. Measurements of velocity were recorded over a one-minute period and then averaged to determine a representative velocity at each sampling interval. The time between sampling intervals is given in Table 3.2. The times given in the table include the minute of recording time.

Table 3.2 Sampling scheme for velocity measurements.

Sampling From (min)	Sampling To (min)	Time Between Measurement Episodes (min)
0	45	2
45	90	5
90	150	15
150	210	30
210	360+	60

In a selected number of experiments transverse transects of velocity and depth-to-bottom were measured, once a stable state had been reached. Transects were measured immediately downstream of the constriction, as well as a sufficient distance downstream that the constriction should no longer have had a

significant effect. A number of velocities were also measured along an upstream transect, to compare velocities before and after the constriction.

Once quasi-equilibrium had been obtained, the flow was stopped and the bathymetry in the flume surrounding the constriction was measured. The system was assumed to be in a quasi-equilibrium state when velocity in the constriction was relatively constant and sand movement was minimal.

3.2.3 Bathymetry Measurements

The bathymetry was measured using a laser scanner with a specified grid spacing of 1mm by 20mm. The scanner transmitted the data directly to a controlling computer. Output was in the form of voltage from the laser, which was then converted to distance using a calibration curve. The scanner is pictured in Figure 3.6.

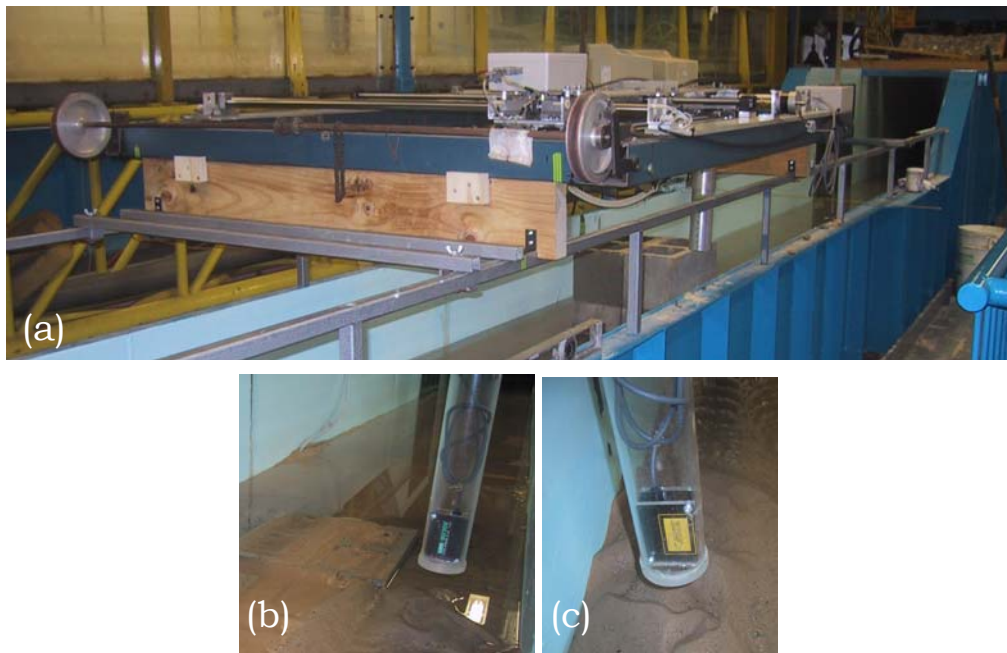


Figure 3.6 (a) The top moving mechanism of the scanner, (b) and (c), the laser measuring part of the scanner, measurements were taken while the flume bed was still submerged.

Measurements were taken by first positioning the scanner at the edge of the flume, as close to the constriction wall as allowed by the plastic tube surrounding the laser, without the tube contacting the constriction. The scanner was then programmed to take measurements at 1mm intervals in a longitudinal run for the 1m of the frame length. Once a longitudinal transect was completed, the scanner was repositioned, 20mm in the transverse direction and another longitudinal transect was completed. In total 41 longitudinal transects were

measured for each experiment. Due to the size of the constriction and its effect downstream, two sets of longitudinal transects were taken to gain data from an area two metres long by 900mm wide. A C++ program was developed to combine the two data sets in the correct place and refine the raw data into a grid set of 10mm longitudinally by 20mm transversely over the entire sample area.

3.2.4 Channel Constriction Results

A number of experiments were performed with a flat bed, in a flume containing a constriction, under similar conditions for repeatability. A typical output plot from one of the runs is shown in Figure 3.7 (Experiment One).

A number of features are evident from the plot. As expected, material was eroded from the throat section and deposited downstream where the velocity and therefore the sediment carrying capacity was reduced.

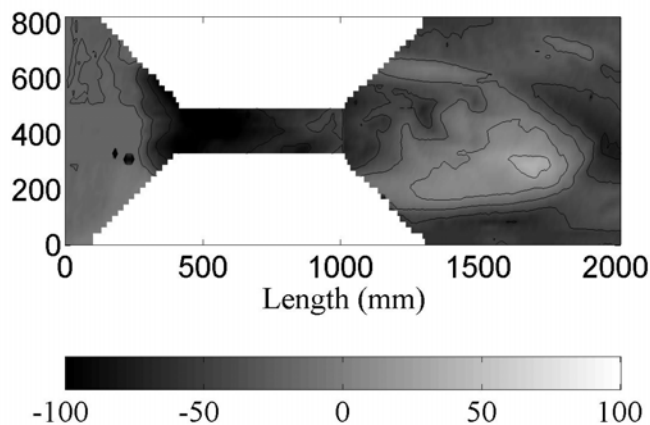


Figure 3.7 Contour plot of a typical channel bed. The contours are plotted at 25mm intervals. The flow was from left to right.

Experiment Two was undertaken with a relatively low flow velocity, one that was only just able to move sediment in the constriction. Only a small, rippled deposition mound formed downstream as can be seen in Figure 3.8.

In Experiment Three (Figure 3.8) the largest flow rate of the six constriction experiments was used. The mound formed downstream and was more drawn out than in other experiments. There were also ripples present downstream.

To assess repeatability, a second experiment (Experiment Four) was undertaken with conditions similar to that of Experiment One. A comparison of the resultant morphology obtained in Experiment One and Four is given in Figure 3.9. The black contours of Experiment One have been superimposed over the greyscale colour-map and white contour lines of Experiment Four. As can be seen in this

Figure, the main deposition mound is in a similar position, as is the start of the erosion, upstream of the main constriction section.

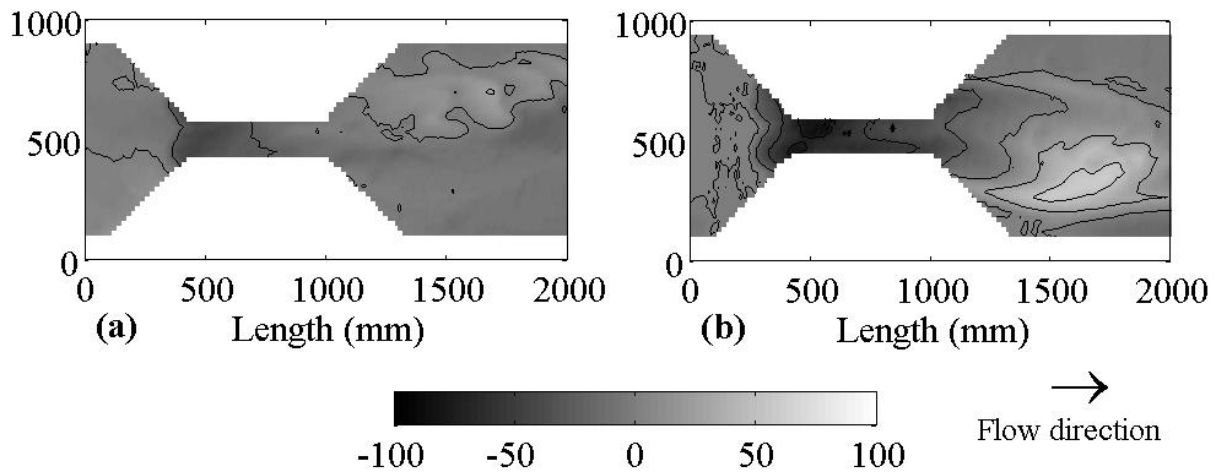


Figure 3.8 Contour plot of (a) Experiment Two results and (b) Experiment Three results.

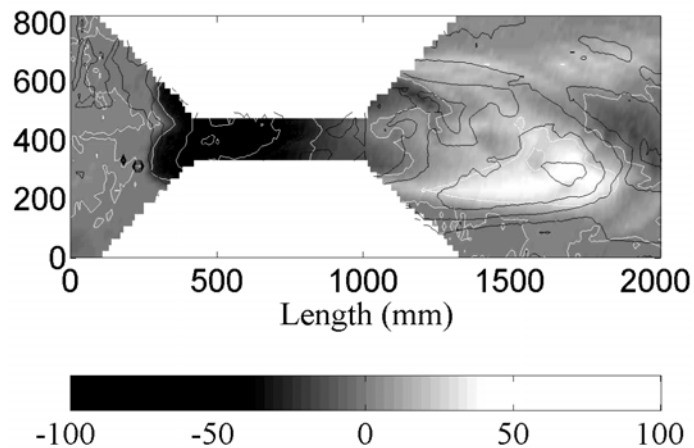


Figure 3.9 Comparison of Experiment One (black) and Four (white). Contours are at 25mm intervals.

Experiments Four and Five gave similar results, but the wall-jet like flow caused the mounds to form on opposite sides of the flume (refer to the morphologies of these experiments in Figure 3.10). The wall-jet like flow refers to the flow exiting the constriction forming a jet that attaches to the side of the flume in a similar way to flow under a sluice gate. This increases the velocity of the flow on one side of the channel, while there is very little flow on the other side. Krampa-Morlu and Balachandar (2001) observed a wall-jet like flow in laboratory experiments around a suspended plate, as did Kells et al. (2001) in flow through a channel, beneath a sluice gate.

A number of scans were undertaken longitudinally, over the area surrounding the constriction, to ensure that the bed morphology was relatively flat. These gave an average bed elevation of $\pm 10\text{mm}$.

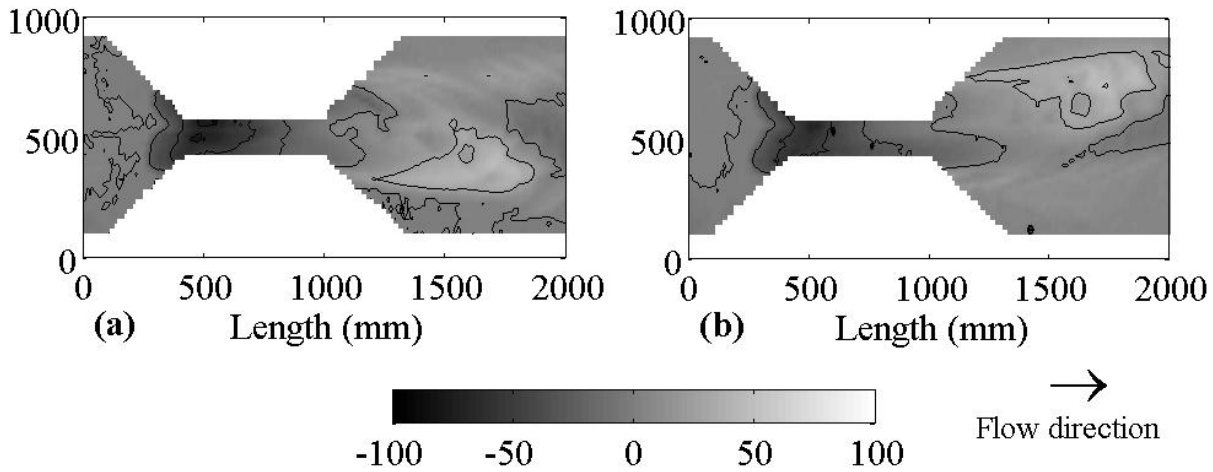


Figure 3.10 Contour plot of (a) Experiment Four results and (b) Experiment Five results.

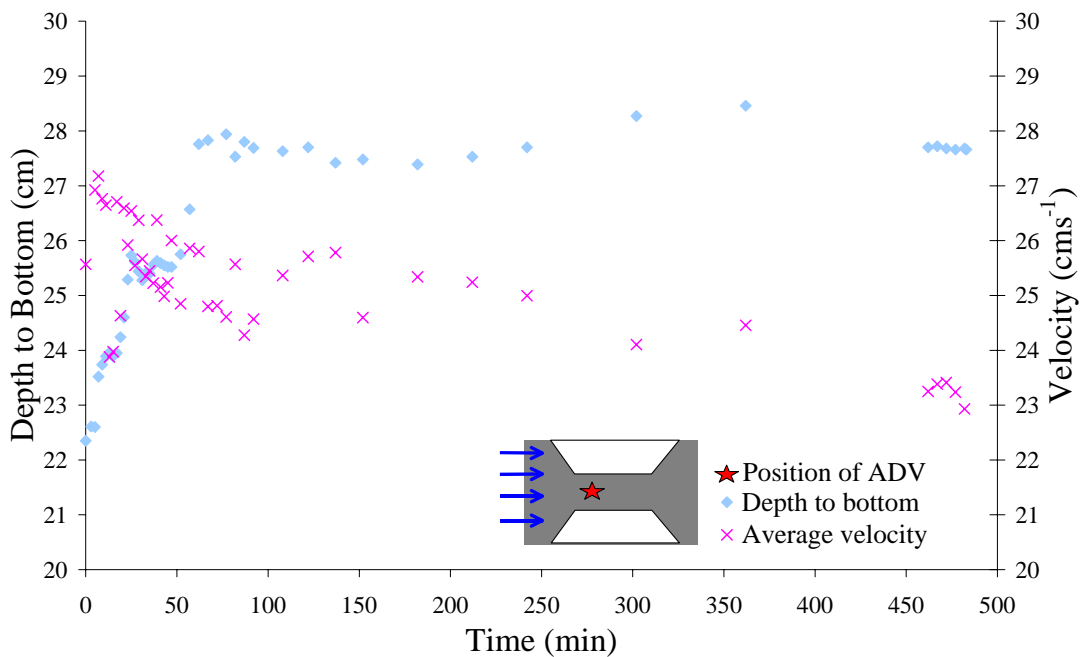


Figure 3.11 Variation of depth to bottom and point velocity (averaged over a one minute interval) with time for Experiment Five.

Figure 3.11 shows that in Experiment Five, in the centre of the constriction, the depth to the bottom steadily increased, before becoming stable after approximately one hour. After this time only slight variations in depth were observed. During the initial stages of the experiment, the point velocity decreased inversely to the increase in depth. It then reached a plateau but

continued to have a slightly downward trend. Velocities were measured using the ADV at varying depths, with measurements averaged over a one minute time interval.

Three velocity transects were obtained from Experiment Six after the system had reached a quasi-equilibrium state. The depth to bottom and velocity trends from these transects are shown in Figure 3.12.

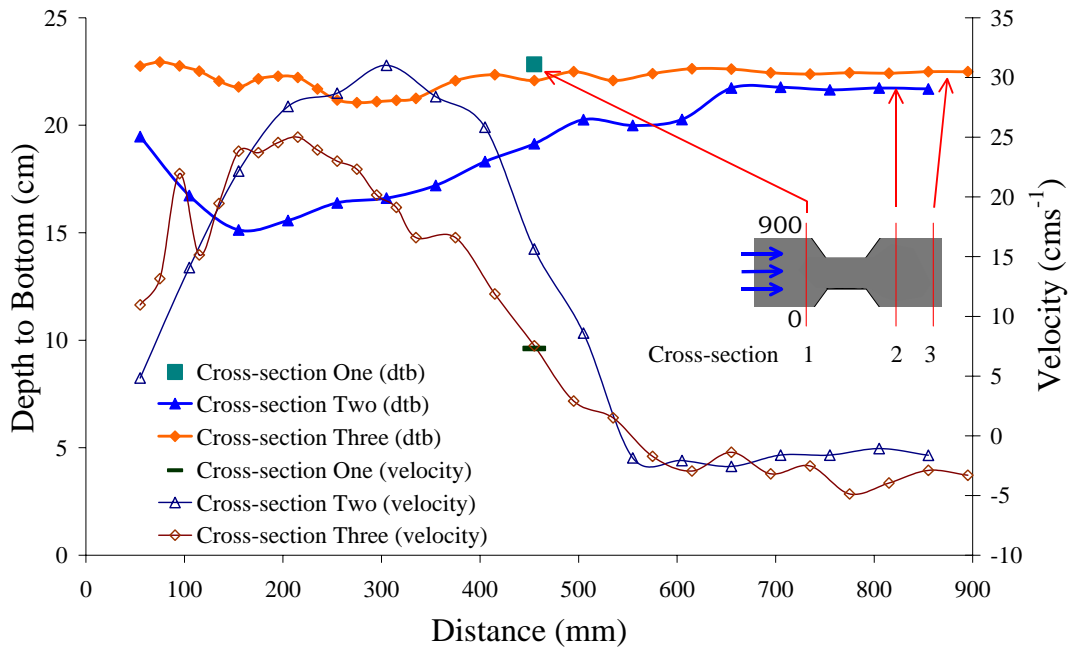


Figure 3.12 Variation of depth to bottom and average velocity across the flume for Experiment Six.

This Figure clearly shows the wall jet like flow. In Transect Two, immediately downstream of the constriction, there is a mound on the left side of the channel, and a flat area on the right side of the channel. In Transect Three the bottom surface is reasonably level and at the same depth as Transect One before the constriction (see Figure 3.12), so the constriction is no longer having an effect on sediment erosion and deposition in this area. However, there is a large difference in velocity between the left and right side of the channel. This suggests that although downstream, the constriction no longer causes erosion or deposition, its effect on velocity and the creation of a wall jet like flow is still felt. The creation of a wall-jet like flow is a reflection of self-organisation and positive feedback within the system, as the system continues in a random path, further strengthening the wall-jet like flow and enhancing the growing mound, rather than negatively affecting the side mound and moving it more to the centre. The random irregularities help to define and self-organise the system into a non-symmetrical pattern. To overcome this wall-jet like flow, a wider flume is

required. However, the purpose of these experiments was to provide some data for comparison with the developed modelling methods.

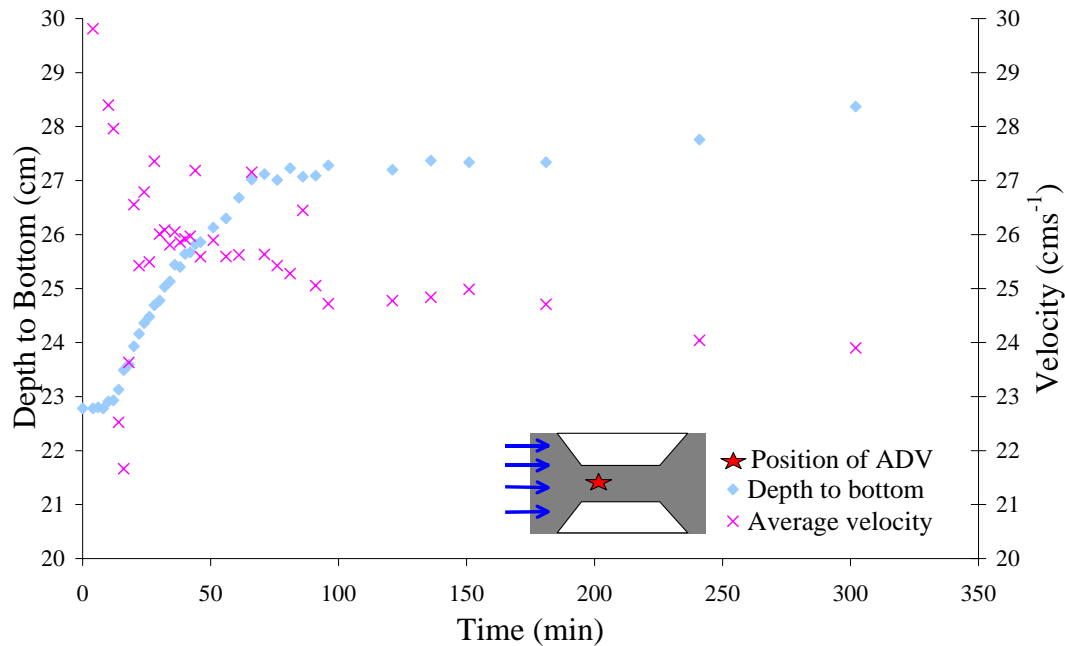


Figure 3.13 Variation of depth to bottom and average velocity with time for Experiment Six.

The variation of depth to bottom and velocity with time is shown in Figure 3.13. As can be seen, the system initially increased depth rapidly in the centre of the constriction. After approximately 70 minutes, a quasi-equilibrium depth was reached. This depth then increased slightly to reach a second, deeper plateau depth after 300 minutes. There was a decrease in velocity initially, which levelled out shortly after a quasi-stable depth was reached.

Table 3.3 Measured water depths and flow rates with corresponding calculated velocities.

Run Number	Upstream Water Head (m)	Downstream Water Head (m)	Flow Rate (m ³)	Velocities	
				Upstream (cms ⁻¹)	Downstream (cms ⁻¹)
One	0.267	0.277	0.0231	9.47	9.12
Two	0.269	0.267	0.0204	8.30	8.36
Three	0.277	0.275	0.0267	10.55	10.62
Four	0.268	0.271	0.0231	9.43	9.33
Five	0.266	0.266	0.0219	9.01	9.01
Six	0.268	0.263	0.0226	9.23	9.40

The flow rates, measured water depths upstream and downstream of the flow disruption, and the velocities calculated from these measurements in each experiment are shown in Table 3.3.

Due to the wall-jet like flow experienced in the constriction experiments, the velocity measurements for Experiment Six (see Table 3.4) do not correspond to the predicted point velocities. The point velocities were measured using the ADV at various distances from the channel bed, while the calculated values are depth averaged values.

Table 3.4 Velocities measured when Experiment Six had reached an equilibrium configuration, along transverse transects, as shown in Figure 3.12, using the ADV meter.

Transect One (cms⁻¹)	Transect Two (cms⁻¹)			Transect Three (cms⁻¹)		
455mm	155mm	455mm	755mm	255mm	455mm	655mm
7.31	23.83	7.54	-4.87	23.00	15.64	-1.38

The difference between measured and actual values is due to the wall-jet like flow creating a situation where the channel appeared a lot narrower than it actually was. It appeared narrower as the water with little or no flow on one side of the channel acted as a wall and increased the velocity on the flow side.

3.3 Channel Constriction Case Study: Traditional Process-Based Model Description and Results

In order to make a comparison between the cellular automaton model and a more traditional model, results of the equilibrium morphology associated with a constricted channel, of similar dimensions and sand type to that of the experimental study described in Section 3.2, were obtained using a traditional model called HYDRA3. The conventional process-based, medium-term model consists of a Navier-Stokes flow model together with a sediment transport routine. These were run for a fixed time step and the solution was allowed to develop until it approached equilibrium and changes in the bed reduced to a nominal cut-off value. The hydrodynamic solver was developed by Walker and further details of its application to other problems are available elsewhere (Walker, 1998). It is a two-dimensional depth-averaged hydrodynamic model. It uses a finite difference method with an alternating direction implicit scheme to solve depth-averaged Navier Stokes equations. The model does not allow for wetting and drying, so boundaries are kept constant throughout the model runs. The results of a typical equilibrium morphology obtained for the constriction

experiment using HYDRA3 are shown in Figure 3.14. Grid size, flow and sediment size used in this example are the same as those used in the cellular automata model, as discussed in Section 3.4.

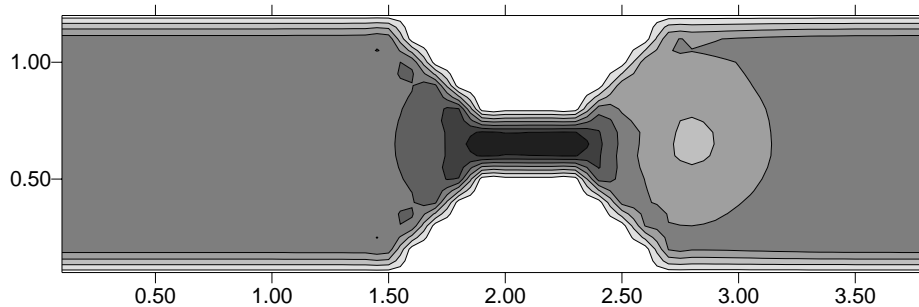


Figure 3.14 Contour plot (at 50mm intervals) of traditional model once simulation had reached equilibrium position. Flow was from left to right.

It is evident from the plot that the pattern of channel erosion is reproduced. However, the deposition of material downstream is not well predicted, as the wall-jet like flow is not taken into account. This is due to the limitation of the hydrodynamic solver, which is depth-averaged. The wall-jet like flow is three-dimensional, and so the vertical attributes are not well defined by the flow solver, hence the flow pattern is more symmetrical than it should be. Due to the wall-jet like flow, no quantitative comparisons were made between the traditional model and the laboratory results. A qualitative comparison shows that the erosion section in the throat of the constriction as predicted by the model is in good agreement with the laboratory findings. The shape of the mound, was more rounded and symmetrical than those observed in the laboratory.

3.4 Channel Constriction Case Study: Cellular Automata Results, Comparisons and Discussion

The cellular automaton model described in Section 3.1 was applied to the constriction test case, using a similar set-up to the one observed in the laboratory as documented in Section 3.2 and modelled using the traditional process-based model as discussed in the previous Section (Section 3.3). This Section gives a summary of a number of key cellular automaton model results and comparisons.

A typical morphological plot of the final profile obtained from the self-organisation model using similar flow and depth conditions to Experiments One and Four is shown in Figure 3.15. Again, as with the process-based model discussed in Section 3.3, the deposition mound was not off to one side as was

observed in the laboratory study due to the wall-jet like flow. However, it was more asymmetrical than the process-based model, forming a more irregular, less rounded mound and so reflects the laboratory results better than the process-based model results. Further comparisons are made between the two modelling methods later in this Section.

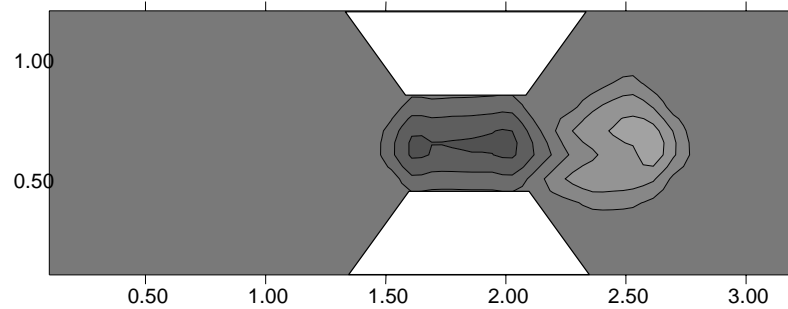


Figure 3.15 Contour plot (at 50mm intervals) of a sample bed morphology resulting from the self-organisation model. Flow was from left to right.

3.4.1 Comparison of Traditional and Self-Organisation-Based Model Results

Further comparisons between the results using a traditional or a cellular automaton model can be made by a comparison of the longitudinal profiles of two results that reflect the majority of morphologies obtained. A comparison plot of the longitudinal cross-sections predicted by both the self-organisation-based and process-based method is shown in Figure 3.16. It can be seen that the cellular automata model predicts a similar depth of the erosion and general position to the traditional model. However, its path to this morphology is quite different, without transport using a sediment transport formula, but rather using physically-based rules, sediment increments and flow directions.

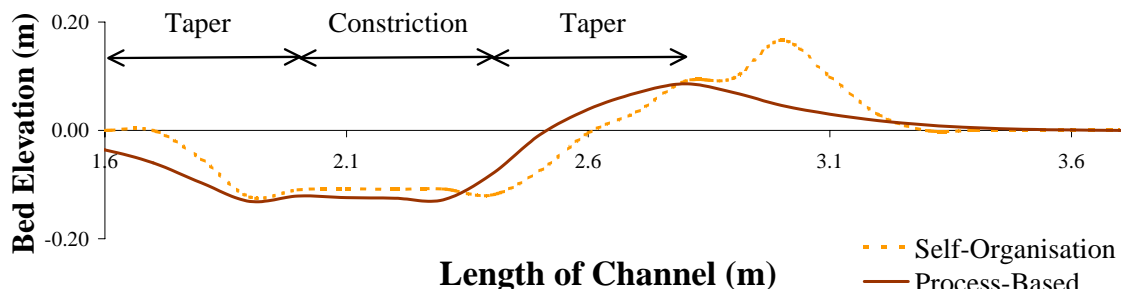


Figure 3.16 Longitudinal cross-section of the channel morphology – a comparison of the process-based and self-organisation-based methods. Flow direction was from left to right.

3.4.2 Comparison of Self-Organisation-Based Model and Laboratory Results

Due to the wall-jet like flow pulling the deposition to one side of the channel, only a qualitative comparison was made between various cellular automata model results and the laboratory findings. A comparison of a model run and the laboratory results of Experiment Two, where both used a similar flow and water depth can be seen in Figure 3.17. In this plot only the area immediately before and through the constriction is compared, as the deposition mound was off-centre in the laboratory study.

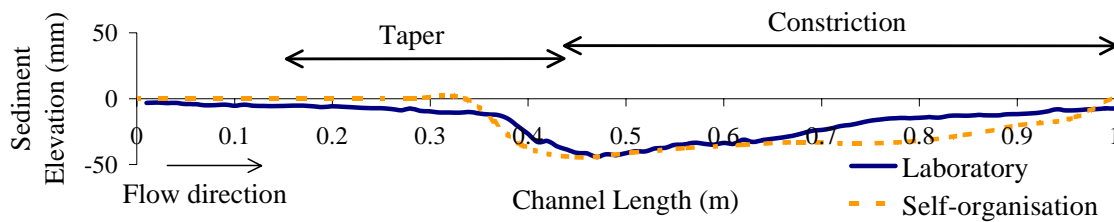


Figure 3.17 Longitudinal cross-section of the channel morphology – a comparison of the self-organisation-based method and laboratory results.

As can be seen in Figure 3.17, the maximum erosion depth in the constriction is predicted well, but is slightly upstream of the laboratory experiment position. There is a slight slope in the initial section of the laboratory experimental results. This may be due to human error in the levelling of the bed. It may also be due to the assumption that the self-organisation rules do not allow any sediment to be moved by the rules unless the velocity criteria is met, rather than there being a gradual inclusion of this rule, with areas where the velocity is almost exceeded having some sediment movement. Another factor that may contribute is the coarseness of the model grid in comparison to the data measured from the experiment, as due to the discretisation and grid capacity of the model, it is not possible to have a gradual movement of sand grains, but only a block of grains moving as one unit.

3.4.3 Sensitivity Analyses: Use of Random Starting Morphology

To test the effect of initial morphology on the resultant morphology, a number of model trials were undertaken. A comparison between the results of two different starting configurations is given in Figure 3.18. It is interesting to note that similar patterns were derived regardless of starting bathymetry, be it random or a flat bed. The area of erosion in particular is very similar. The slight variation is due to the randomness of the bed creating morphologies with slightly different

volumes of sediment. There was less than one percent difference in the energy lost over the channel between runs with different starting configurations. This suggests that the pattern formed is indeed due to a self-organising process, as this type of process is not dependent on the starting configuration (Bolliger et al., 2003).

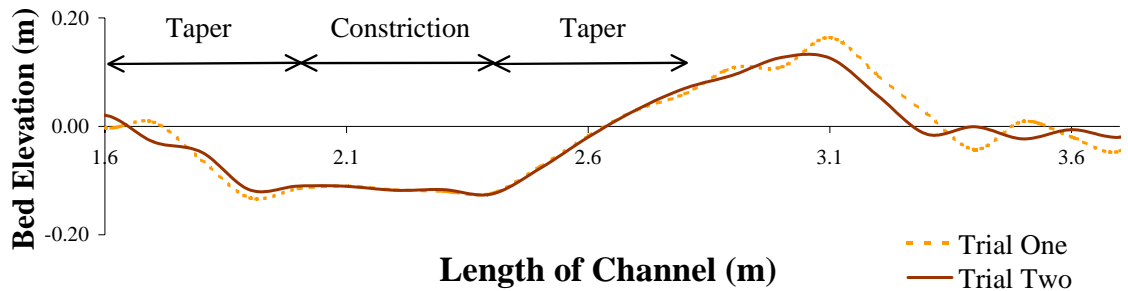


Figure 3.18 Comparison of longitudinal cross-sections from two different random starting configurations. Flow direction was from left to right.

3.4.4 Sensitivity Analyses: Grid Size

A comparison of the differences due to the use of a coarse or fine grid, for the constriction case can be seen in Figure 3.19. The erosion that develops at a quasi-stable state is similar regardless of the grid size used. However, the coarse grid produced a larger, smoother mound. This is due to the larger grid sizes meaning that more sediment is moved in each step. The finer grid better reproduces the experimental results.

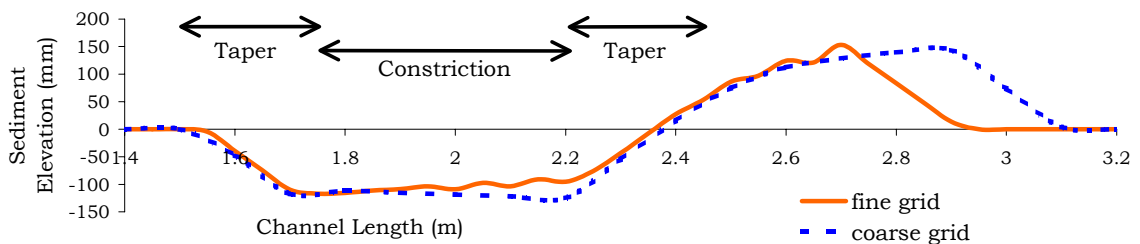


Figure 3.19 Comparison between coarse and fine grid model results through centre of constriction. Flow direction was from left to right.

3.4.5 Sensitivity Analyses: Fixed or Variable Avalanche Criterion

The avalanche criterion was applied in situations where the angle of repose was exceeded. Avalanching occurred to bring the cells in question back to the either a fixed maximum angle of repose or a variable angle, randomly chosen between

specified limits. These specified limits were chosen to be between fifty percent and one hundred percent of the maximum angle of repose.

A comparison between fixed avalanche angle and random avalanche angle is shown in Figure 3.20. As this Figure shows, the differences in quasi-stable morphology are small overall as the same general shape is obtained, however, with the variable avalanche rule the morphology is smoother, less extreme and better able to reproduce the experimental results. This suggests that this rule is important in producing a morphology more akin to channel morphologies in nature.

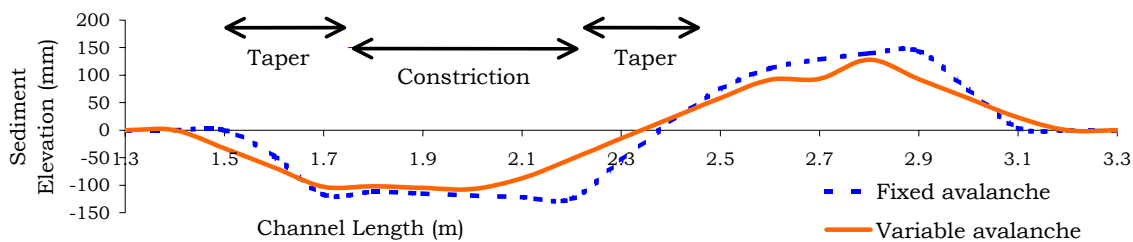


Figure 3.20 Comparison of model runs with different avalanche mechanisms. Flow direction was from left to right.

3.5 Channel Obstruction Case Study: Laboratory Method and Results

A number of further investigations were undertaken using a channel obstruction as an experimental example. In this situation erosion occurred between the obstruction and the channel walls, with deposition downstream of the erosion holes. A description of the case study is shown in Figure 3.21.

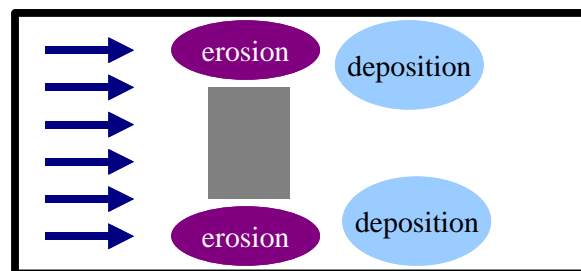


Figure 3.21 Obstruction case study description.

In a similar fashion to the constriction case study, a number of laboratory experiments were undertaken in a flume and results of a traditional model and the self-organisation-based model were compared to the measured morphologies.

The experiments were undertaken in a flume approximately 10m long, and 0.914m wide, that contained an obstruction in its centre. A diagram of the experimental set-up can be seen in Figure 3.22.

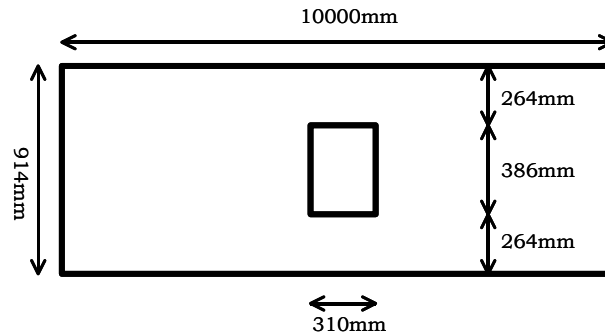


Figure 3.22 Obstruction laboratory set-up.

In the centre of the flume a concrete obstruction was placed, being 386mm wide and 310mm long, with flow in the flume reduced to 264mm on either side of the obstruction. Pictures of the obstruction before experiments were undertaken and during the experiments are shown in Figure 3.23. Two flow rate and depth combinations were chosen for the experiments so that the bed surrounding the obstruction was subjected to clear water scour. These are shown in Table 3.5.

Table 3.5 Flow characteristics of laboratory experiments.

Laboratory Experiment	Flow Rate ($\text{m}^3 \text{s}^{-1}$)	Flow Depth (m)
One	0.0577	0.314
Two	0.0444	0.296



Figure 3.23 The obstruction in the rectangular flume, before and during experiments.

The bed was composed of fine sand with a d_{50} of $240\mu\text{m}$. Before each experiment the bed was flattened and levelled to create a negligible bed slope in both the

longitudinal and transverse directions. The flume was gradually filled with water, with care taken to ensure the sand on the bed was not disturbed. Once water in the flume reached an acceptable level, the flow was increased to the desired rate and the system left to attain an equilibrium morphology. After a few hours there was very little bed change. Measurements of the bed morphology and velocity profiles were made after the system had been left for approximately six hours and no further velocity or depth changes were observed in the area surrounding the obstruction. Measurements of velocity and depth to bottom were taken during the experiment using an ADV meter on one side of the obstruction, to determine when the system had reached a stable morphology. These measurements for Experiment One are shown in Figure 3.24. It can be seen that the velocity decreased initially as the system self-organised itself, and then reached a constant rate after approximately an hour and a half.

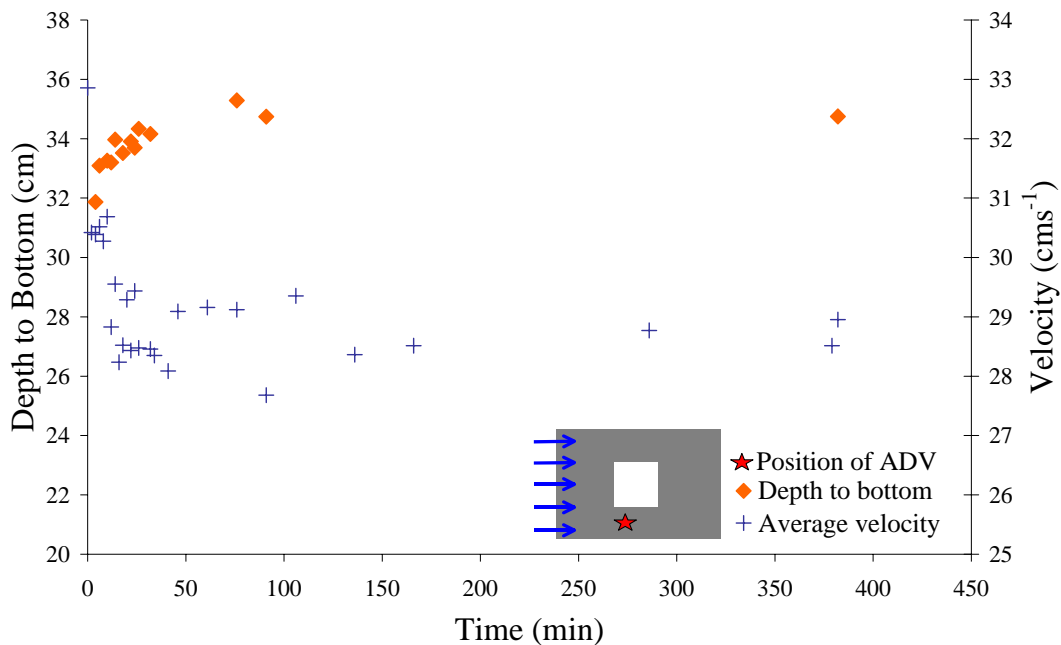


Figure 3.24 Depth to bottom and velocity measurements from Experiment One, each point represents an average of values recorded over a one minute time period, measured using an ADV, positioned to the right of the obstruction (facing down flow).

Figure 3.25 shows the velocity profiles measured after six hours along three different cross-sections in the channel. The velocities approximately 1.5m upstream and 2m downstream of the obstruction (Cross-Sections One and Three) are quite similar, suggesting that the obstruction only influences a small area of the channel, immediately surrounding it. The velocity profile 300mm immediately downstream of the obstruction (Cross-Section Two) shows the velocity pattern of flow towards the obstruction in the lee of the obstruction and

increased velocity over the deposition mounds. Unlike the constriction example discussed in Section 3.2, there appeared to be no wall-jet like flow in this configuration, with the deposition mounds being pulled to each side equally.

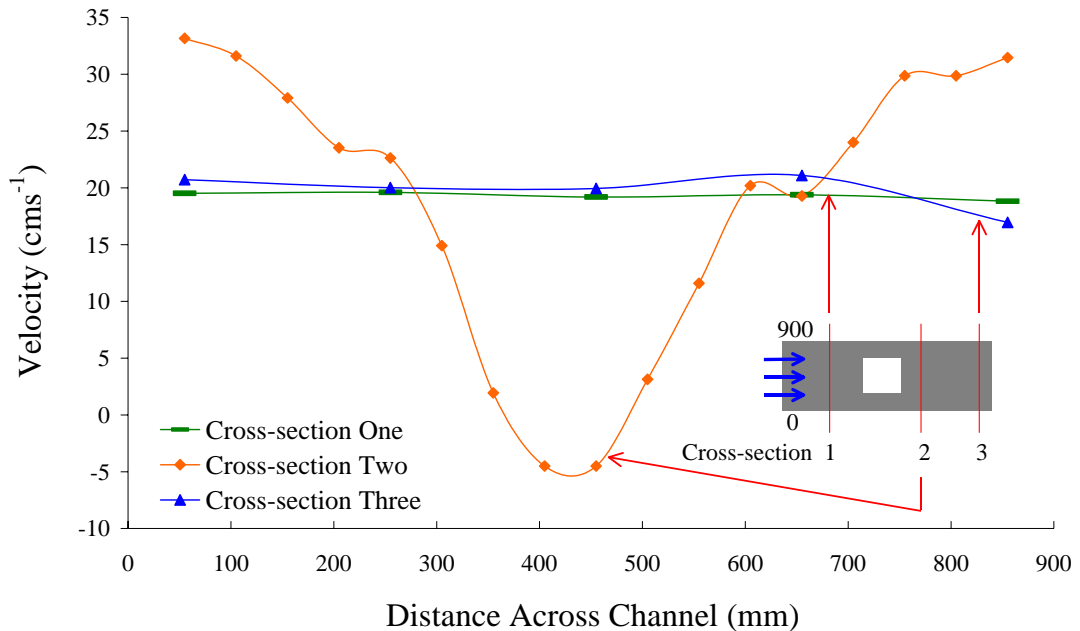


Figure 3.25 Velocity profiles at equilibrium for Experiment One.

Bathymetry measurements were taken once the flow had been stopped, and were measured using the same laser scanner used in the constriction experiments discussed in Section 3.2. Measurements were taken using a grid spacing of 10mm by 20mm with a vertical accuracy of $\pm 0.2\text{mm}$.



Figure 3.26 The resultant morphology in the channel from Experiment One, looking upstream and downstream respectively. The water and upper parts of the obstruction have been removed.

The resultant morphology for Experiment One is shown in Figure 3.26. There are a number of visible morphological characteristics associated with the obstruction. Sand was eroded on either side of the obstruction where velocity

and therefore sediment carrying capacity was increased. This sand was then deposited downstream of the obstruction on either side of the channel where velocities and sediment carrying capacities were reduced.

Table 3.6 Measured water depths and flow rates with corresponding calculated velocities.

Run Number	Upstream Water Head (m)	Downstream Water Head (m)	Flow Rate (m ³)	Velocities	
				Upstream (cms ⁻¹)	Downstream (cms ⁻¹)
One	0.319	0.308	0.0577	19.79	20.50
Two	0.299	0.292	0.0444	16.25	16.64

Table 3.7 Velocities measured after formation of equilibrium morphology along transverse transects, as in Figure 3.25, using the ADV meter.

Run Number	Transect One (cms ⁻¹)			Transect Two (cms ⁻¹)			Transect Three (cms ⁻¹)		
	55mm	455mm	655mm	155mm	455mm	755mm	255mm	455mm	655mm
One	19.52	19.19	19.38	27.92	-4.50	29.87	20.01	19.94	21.09
Two	15.66	15.81		27.09	-2.37	27.92	17.54	15.55	18.68

From a comparison of Table 3.6 and Table 3.7 it can be seen that for Experiment One, the initial velocity upstream of the obstruction is measured at 19.1cms⁻¹ while it is estimated from the flow and depth measurements as 19.8cms⁻¹. Downstream of the obstruction, the ADV measured the centre-line velocity to be 19.9cms⁻¹ while the flow and depth measurements estimated it to be 20.5cms⁻¹, which shows that the depth and flow approximations are relatively accurate. Similar comparisons can be made for the velocities obtained in Experiment Two.

3.6 Brier Skill Score Definition

Part of the research was the validation of the numerical models quantitatively, by comparing traditional process-based models to the self-organisation based models, using the results from a number of laboratory experiments. This is important as it shows that the predicted patterns are in fact similar to those obtained under real conditions. Miao et al. (2001) and Pannell et al. (2002) obtained self-organised ripple type patterns that appeared similar to those in the field, but detailed comparisons were not made. This trend is similar in much of the self-organisation research; patterns are generated, but not verified in detail. Favis-Mortlock (1998) is one example of where a laboratory study was undertaken and showed promising qualitative comparisons, with a scale laboratory model of rills developing on a hillside predicting similar paths to that of the self-organisation model. Little work has been undertaken to the authors' knowledge, comparing self-organisation models and more traditional models

quantitatively to laboratory or field studies. In this Chapter comparisons are made between laboratory and self-organisation-based model results using the Brier Skill Score to compare the morphologies quantitatively (see Section 3.8).

The Brier Skill Score is a method that can be used to compare how well shapes are predicted. It was originally developed by meteorologists to compare atmospheric pressure distributions, and has recently been applied in coastal morphological research (van Rijn et al., 2003; Sutherland et al., 2004). It gives an indication of the bias, accuracy and skill associated with the models and compares them to an initial or baseline condition, so that the size of area sampled and inclusion of unchanged areas, does not affect the result. Bias is often measured as the similarity of the models' means. Accuracy is the average error between the two models. Skill is the accuracy of the model in predicting the desired result relative to a baseline or initial condition. For example, a positive skill level would predict an increase in bed elevation if that is the change observed in the field, but a negative skill level would result if the numerical model predicted a decrease in bed elevation relative to the initial elevation, even if the resultant shape was still accurate, but on a different baselevel (Sutherland et al., 2004). This is illustrated in Figure 3.27. The Brier Skill Score is a better determination of model predictability as it considers the significance of correlated values, rather than just the correlation coefficients (Murphy and Epstein, 1989). It is able to determine skill, whether a shape is accurate with regard to its movements from a baseline, rather than whether two trends correlate with each other.

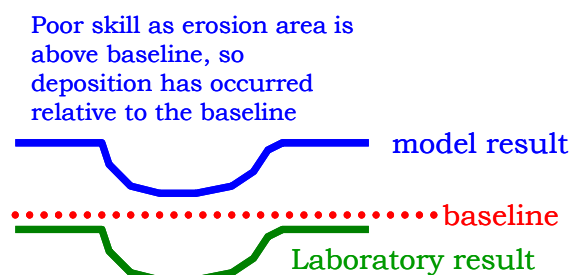


Figure 3.27 Illustration of a negative skill model result, in relation to a baseline measurement.

The Brier Skill Score predicts a number between 1 and negative infinity. A value of 1 suggests perfect model and laboratory similarity, a value of 0 signifies that the results correspond to the baseline values and no change has occurred, while a negative value corresponds to a negative skill score, where the model results have moved from the baseline in the wrong direction compared to the laboratory results. Use of the Brier Skill Score is still in its infancy in morphological

modelling fields, and more research is needed into the exact meaning of different score values. However, Sutherland et al. (2004) suggest that as a rough guideline a score above 0.5 represents an excellent agreement and above 0.1 reasonable (see Table 3.8).

Table 3.8 Brier Skill Score interpretation guidelines (after Sutherland et al., 2004).

Relative Performance of Model	BSS Value Obtained
Excellent	1 - 0.5
Good	0.5 - 0.2
Reasonable/fair	0.2 - 0.1
Poor	0.0 - 0.1
Bad	< 0.0

The Brier Skill Score is calculated using the mean squared errors (*MSE*) of the laboratory measurements (*X*) and the numerical model predictions (*Y*), compared to the initial or baseline laboratory measurements (*B*), as shown in Eq. (3.2).

$$\text{Brier Skill Score} = 1 - \frac{MSE(Y, X)}{MSE(B, X)} \quad (3.2)$$

It can also be broken down into a number of components which suggest where the model errors may occur.

3.7 Channel Obstruction Case Study: Traditional Process-Based Model Description and Results

The obstruction problem was analysed using the same traditional process-based medium-term morphological model as was used to model the constriction problem, as detailed in Section 3.3. The model consisted of a Navier-Stokes flow model and a sediment transport routine. The equilibrium morphology was determined when the model had been applied over a period of time and the bed changes reached a nominal cut-off value. For comparison purposes, the Figure shown below uses similar grid size, flow and sediment attributes as the fine grid cellular automata model discussed in Section 3.8 (Figure 3.29). As can be seen in the contour plot of the model in Figure 3.28, the erosion and deposition pattern is poorly represented. The difference in total area compared is due to the instrumentation casing, which prevented the laser scanner from measuring within 2cm of any solid fixed object. The obstruction was removed from the

channel to facilitate ease of measurement, but the morphology close to the flume walls could not be measured.

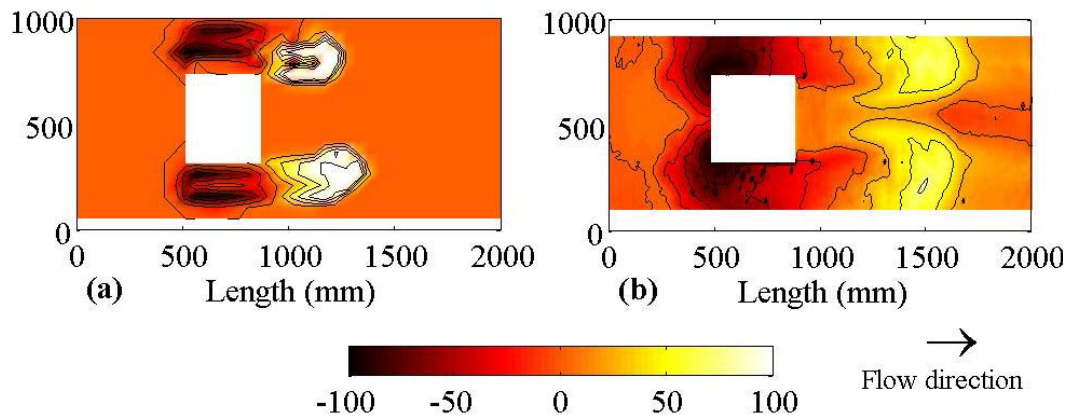


Figure 3.28 Morphology of the channel bed surrounding an obstruction obtained from (a) the traditional model, and (b) laboratory Experiment One. Flow was from left to right. Contour lines are at 25mm intervals.

The correlation coefficient between corresponding laboratory and numerical model longitudinal-sections is 0.33, but the Brier Skill Score is a value of -0.63 . The reason for this poor result is the misalignment of the depositional mounds in the numerical model. The depositional mounds are placed too close to the obstruction and grow too high with respect to the laboratory results, possibly as a result of the model ignoring the effect of bed slope on sediment transport.

3.8 Channel Obstruction Case Study: Cellular Automata Results, Comparisons and Discussion

The cellular automaton model, discussed in Section 3.1, was applied to an obstruction setup, similar to the laboratory experiments detailed in Section 3.5, with similar flow, depth and grain size. A comparison of the equilibrium morphology obtained from a typical cellular automaton model run and the laboratory results of Experiment One is shown in Figure 3.29. The model was able to represent the erosion and depositional areas well. The model depositional mounds were similar in shape to the laboratory results. The self-organisation based model has a correlation coefficient between corresponding laboratory and model morphologies of 0.74. It has a Brier Skill Score of 0.34, which according to Sutherland et al. (2004) means that the self-organisation model gives a good representation of the laboratory results (see Table 3.8). This method gives a much better agreement with laboratory results than the traditional model.

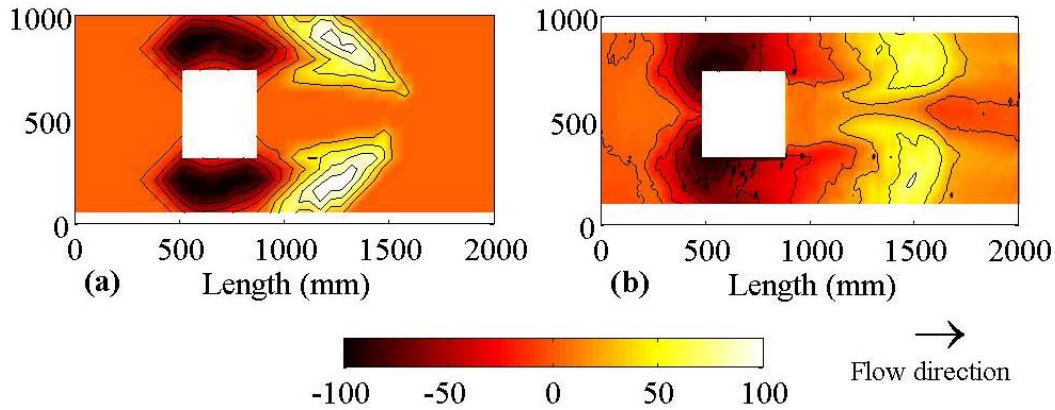


Figure 3.29 Morphology of the channel bed surrounding an obstruction obtained from (a) the self-organisation model, and (b) laboratory Experiment One. Flow was from left to right. Contour lines are at 25mm intervals.

A comparison of the model and Experiment Two is given in Figure 3.30. This result shows that the model clearly predicts the erosion of the channel, but under predicts the extent of the deposition.

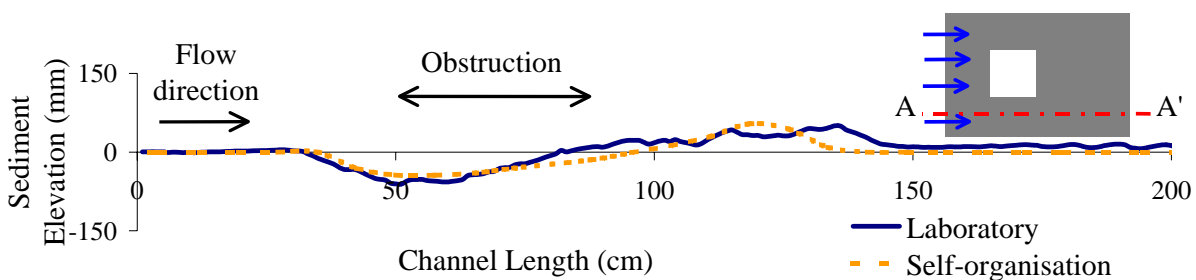


Figure 3.30 Longitudinal cross-section (A-A') comparison of channel morphology obtained from laboratory Experiment Two and the cellular automaton model. Flow was from left to right.

There are a number of possible reasons for differences between the experimental and numerical results. Firstly, the threshold equation depends only on the d_{50} and d_{90} values of the sediment, and may not limit the growth of the mounds accurately, allowing higher mounds to develop numerically. The approach is only as good as the hydraulic model used to determine velocities. This model gives a good approximation of velocities in the system, but it does not determine three-dimensional velocities or the horseshoe and wake vortices that occur around the edges of the obstruction. The use of three-dimensional velocities near the top of the deposition mounds may help to limit the mound heights and may be the reason why the model predicts a higher mound than that observed experimentally. A more accurate turbulence model may help to smooth and limit the growth of the deposition mounds. Three-dimensional velocity modelling was beyond the scope of this research, the objective being to show that realistic

equilibrium morphologies could be predicted using a two-dimensional depth-averaged hydrodynamic solver.

To test the self-organisation numerical model's robustness and the effect of various assumptions, a number of runs were undertaken, varying initial bed morphology, sediment increment size, model grid size, sediment diameter and angle of repose value. The results from these runs are discussed and displayed in the following Section.

3.8.1 Sensitivity Analyses: Random Starting Morphologies

A test of a self-organisation system is the system's non-reliance on starting conditions, as mentioned in Section 3.1. Random variations should produce similar stable equilibrium morphologies. A number of tests were carried out, starting the model with different randomly undulating beds, where initial grid points were given random bed elevations ranging from -50mm to $+50\text{mm}$ below and above a flat bed. The results of four of these tests are given in Figure 3.31.

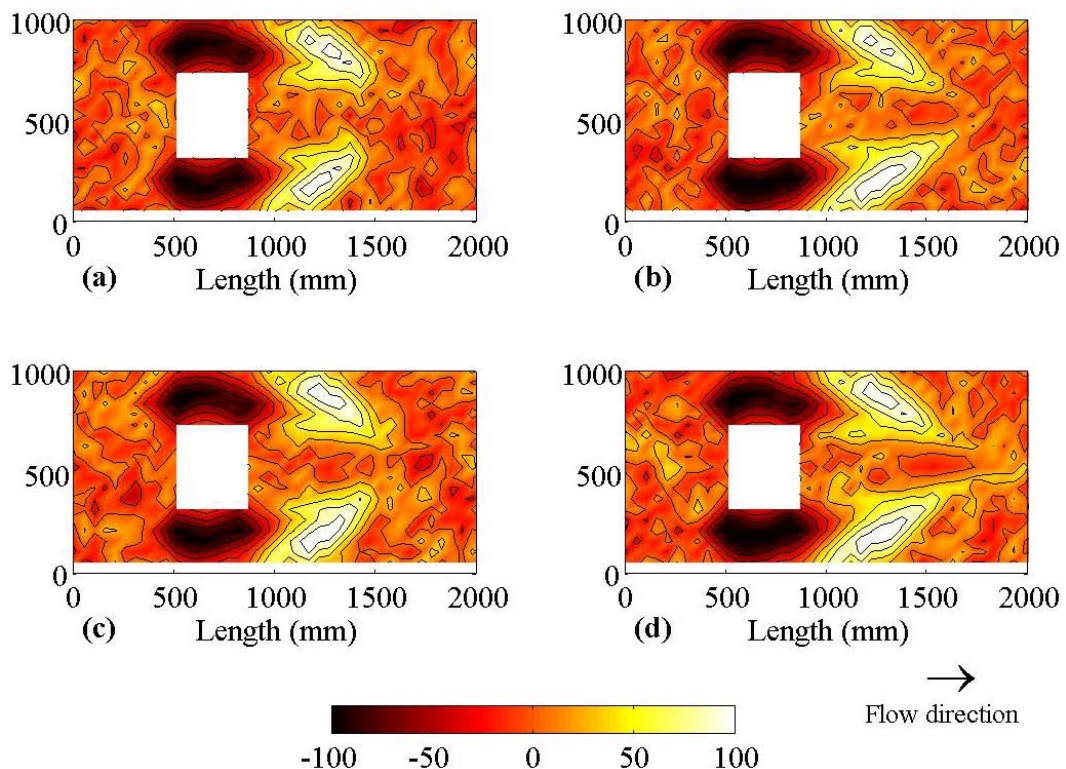


Figure 3.31 Comparisons of channel morphology obtained from different starting morphologies using the self-organisation-based model. Flow was from left to right. Contour lines are at 25mm intervals.

As this Figure shows, regardless of the initial conditions, similar end morphologies were reached, in particular the erosion holes. This suggests that the pattern formed is not dependant on starting conditions and is able to move to a stable, equilibrium morphology. The slight variations between deposition mound morphologies are due to the distribution of the initial sediment, with different amounts available upstream and downstream for bed moulding in the different cases considered.

3.8.2 Sensitivity Analyses: Different Sediment Increment Sizes

A comparison of resultant morphologies formed using different sediment increments is given in Figure 3.32. The Brier Skill Scores for sediment increments of 10mm and 0.5mm were 0.35 and 0.36 respectively. This shows that the equilibrium morphology is insensitive to the sediment increment size used, as similar morphologies form that are in good agreement with the laboratory results, regardless of the sediment increment size. This suggests that the self-organisation model is robust. Smaller sediment increments produce longer run times, so a moderate increment size is favourable as this will minimise run times whilst still allowing the prediction of the overall equilibrium morphology.

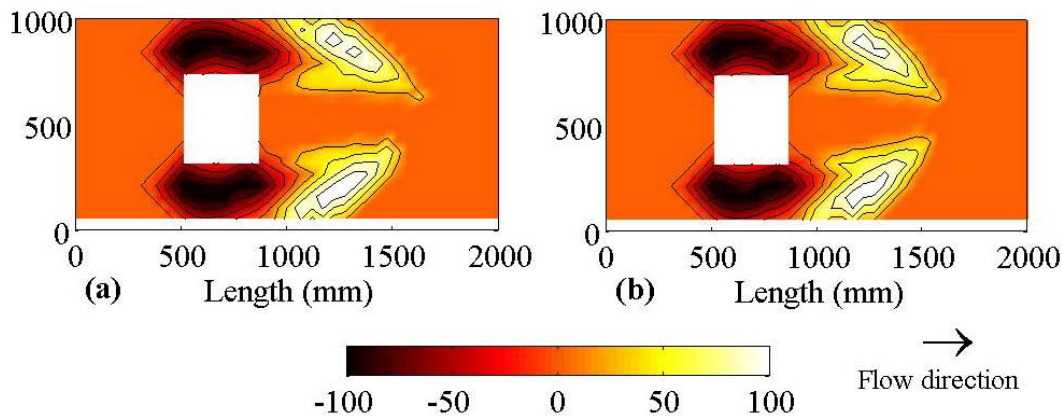


Figure 3.32 Morphology of the channel bed surrounding an obstruction obtained from the self-organisation-based model using two different increment sizes of (a) 10mm and (b) 0.5mm. Flow was from left to right. Contour lines are at 25mm intervals.

3.8.3 Sensitivity Analyses: Different Grid Sizes

A comparison of the results obtained when different grid sizes of 0.1m and 0.05m were used in the model is shown in Figure 3.33. A Brier Skill Score of -0.16 was obtained for the coarser size grid. It can be seen that a finer grid size allows for a more accurate representation of the equilibrium morphology, with a better

prediction of the depositional mound position and shapes. This finer sized grid was adopted for most simulations, giving a model size of 81 by 21 cells in the x and y directions respectively.

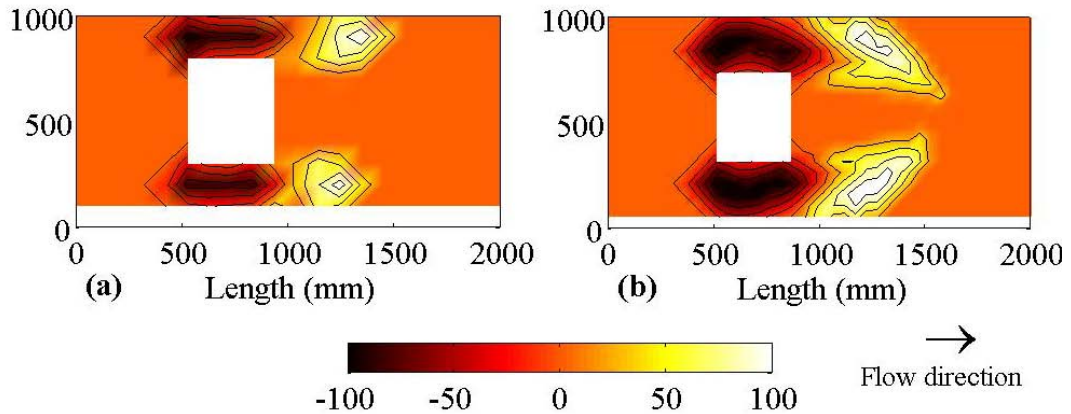


Figure 3.33 Morphology of the channel bed surrounding an obstruction obtained from the self-organisation model using two different grid sizes of (a) 0.1 m and (b) 0.05 m. Flow was from left to right. Contour lines are at 25mm intervals.

3.8.4 Sensitivity Analyses: Fixed or Variable Angle of Repose

The angle of repose exceedance rule was applied to create either a fixed or variable angle of avalanche. When an angle of repose was exceeded, avalanching occurred to bring the cells in question back to a suitable angle. The fixed angle was the maximum angle of repose. The variable angle was chosen as a random value between fifty percent and one hundred percent of the maximum angle of repose. The variable angle of repose rule created a smoother, shallower morphology, similar to the laboratory result of Experiment One (see Section 3.5).

A typical profile from laboratory Experiment One is compared to a profile found in a model run with a fixed avalanche angle, in Figure 3.34.

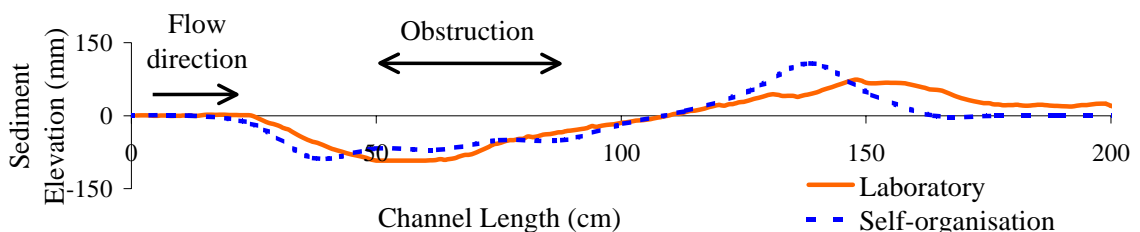


Figure 3.34 Comparison of laboratory Experiment One and self-organisation model with fixed avalanche angle along the right side of the channel facing downstream.

As can be seen in this Figure, the modelled morphologies are similar in parts, as the initial slopes approaching the depression and hump are correct, and the maximum depth and height of the profile are predicted, but the overall shape does not match the experimental results.

When the variable angle rule was used however, the likeness of the experimental and computer-modelled improves remarkably. As can be seen in Figure 3.35, the erosion, deposition as well as angles are all predicted more accurately.

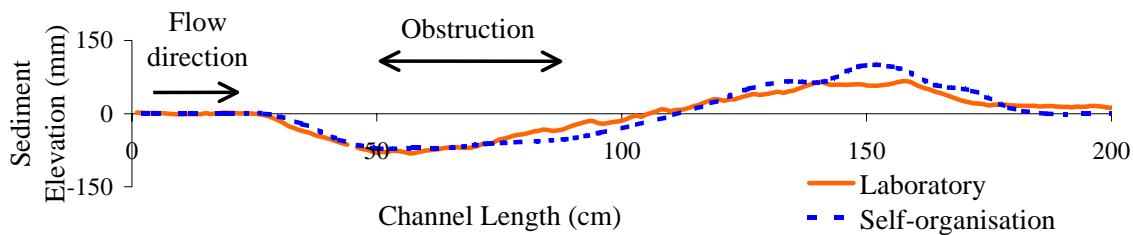


Figure 3.35 Longitudinal cross-section comparison of morphology on the right side of the obstruction (facing flow direction) obtained from the laboratory study and self-organisation-based modelling study using variable avalanche angle.

3.8.5 Sensitivity Analyses: Angle of Repose Value

In general a common critical angle of repose of 35° was adopted. However, to test the effect of altering the critical angle of repose, the basis for one of the self-organisation rules, a number of other critical angles of repose were analysed, the results of some of which can be seen in Figure 3.36.

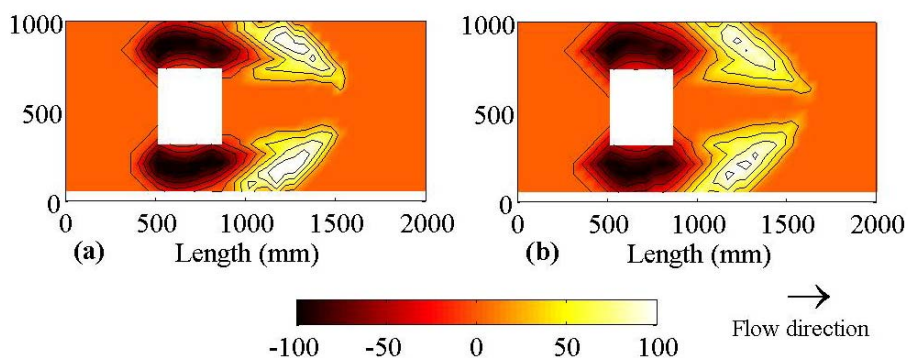


Figure 3.36 Contour plot of different angles of repose (40° (a) and 30° (b)). The contours are plotted at 25mm intervals. The flow was from left to right.

The results of this analysis are as expected, for a greater critical angle of repose, as shown in part (a), the mounds may consist of steeper sides, and so may build up to a greater height. In the case of a lesser critical angle of repose, the mounds

will be shallower and wider to account for the stipulation of lesser gradient on their side slopes. The effect of differing angles of repose is also noticed to a lesser extent in the erosion holes, with sides being less and more steep, creating larger and smaller holes with lesser and greater angles respectively.

3.8.6 Sensitivity Analyses: Sediment Grain Size

In nature, it is unusual that a system would consist of completely uniform sediment of a single grain size. In order to analyse the effect of different grain sizes on the self-organisation model, which relies on the use of grain size to calculate critical velocity, a number of runs were undertaken using various grain sizes smaller or larger than the d_{50} of the laboratory sand. The results of these runs can be seen in Figure 3.37. In part (a) it can be seen that finer sand allows for a more diffused deposition pattern, with sediment mounds stretched out further down stream. In the case of coarser sediment (see part (d)), the mounds appear blunter and more compact, with less transport downstream, as higher critical velocities are required to transport the sediment.

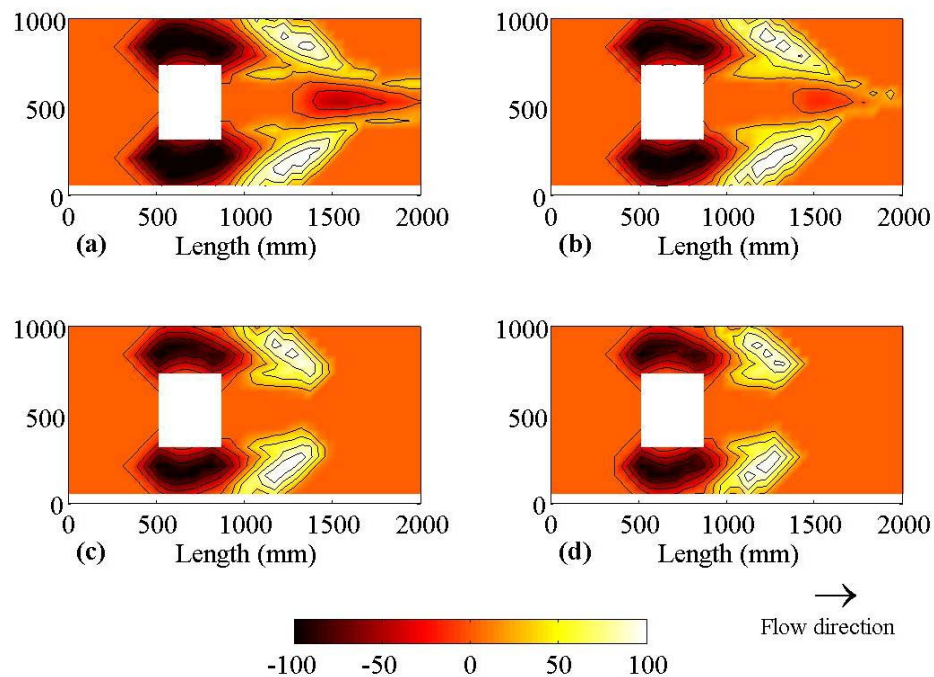


Figure 3.37 Contour plot of different d_{50} sizes ($140\mu\text{m}$ (a), $200\mu\text{m}$ (b), $280\mu\text{m}$ (c) and $340\mu\text{m}$ (d)). The contours are plotted at 25mm intervals. The flow was from left to right.

3.8.7 Rule Violations Pattern

Initially, when the self-organisation process starts from a flat bed, the cells in the area to either side of the obstruction have velocities that are greater than the

critical velocity, so a large number of sediment increments are moved to adjacent cells. As the process progresses, the areas where velocity exceeds critical velocity are reduced, and the number of sediment increments moved in each iteration step decreases. As more increments have built up in areas below critical velocity, the number of critical angle of repose violations increases. However, towards the end of the simulation, the number of sediment increments moving in each iteration is reduced, so the potential for a critical angle of repose violation is also reduced. This can be seen in Figure 3.38. This Figure is a good illustration of the existence of feedback in the simulation. Without the critical velocity rule, and feedback between the morphology and the new flow field that it creates, sediment would be dumped indefinitely in a vertical pile just outside the area of active erosion, where the initial velocity is no longer above the critical velocity. However, the critical angle of repose rule forces the mounds to stop growing and the holes to stop eroding, when the side angles are greater than the angle of repose, creating avalanches. The feedback between the morphology and the flow, where new flow fields are generated with changes in morphology is also necessary, since without this feedback, the zone where critical velocity is exceeded would not change.

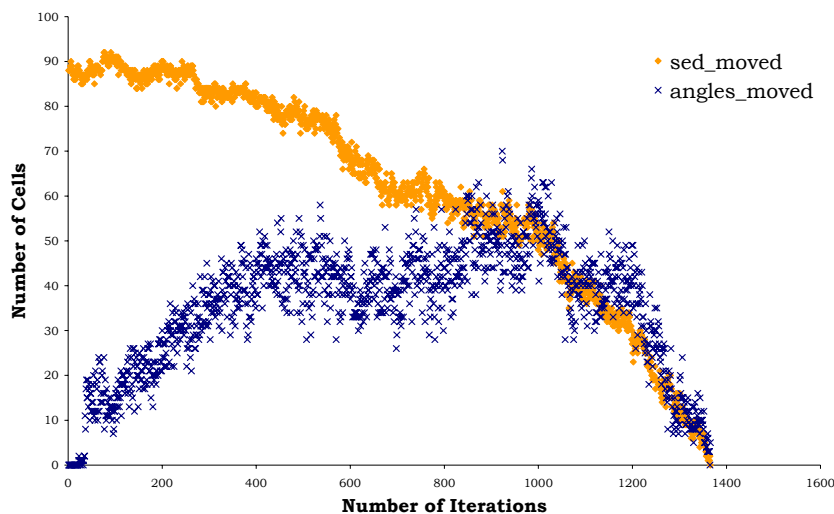


Figure 3.38 Path of self-organisation model for Experiment One set-up. Number of cells in which sediment increments are moved in each iteration and number of cells where avalanching occurs.

3.8.8 Comparison of Laboratory Velocities and Hydrodynamic Model Calculations

A check was made of the calculations of the 2DH hydrodynamic model depth averaged velocities compared to the physical near bed velocity measurements. The velocities modelled in the channel around the obstruction, using the actual

laboratory bed morphology were determined using the HYDRA3 model (the workings of which are discussed in Section 3.3). A comparison plot of the model depth averaged velocities compared to the actual near bed velocities are given in Figure 3.39 to Figure 3.44 based on the morphologies that resulted in Experiments One and Two respectively.

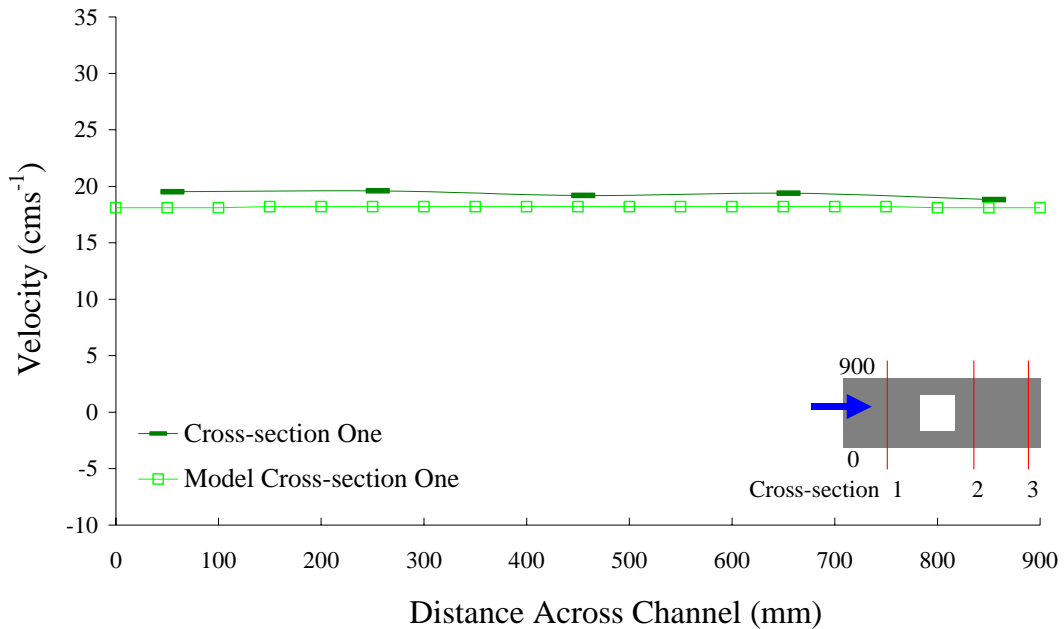


Figure 3.39 Comparison of depth averaged velocity field obtained from model morphology and that measured near the bed in laboratory Experiment One, upstream of the obstruction.

As can be seen by these results, the initial velocity predictions of Cross-Section One, before the obstruction, are quite similar to the measured results. The measured results are point measurements at an instantaneous depth however, while the model predicts a depth averaged velocity, so the magnitudes are not expected to agree directly, rather the trend between modelled and observed should be similar.

A comparison of Cross-Section Two shows that the model replicates the general trend of higher velocities on either side, and lower velocities in the centre of the channel. The edge effects were not measured in the physical experiment, so a comparison between the model and laboratory is not possible in this area.

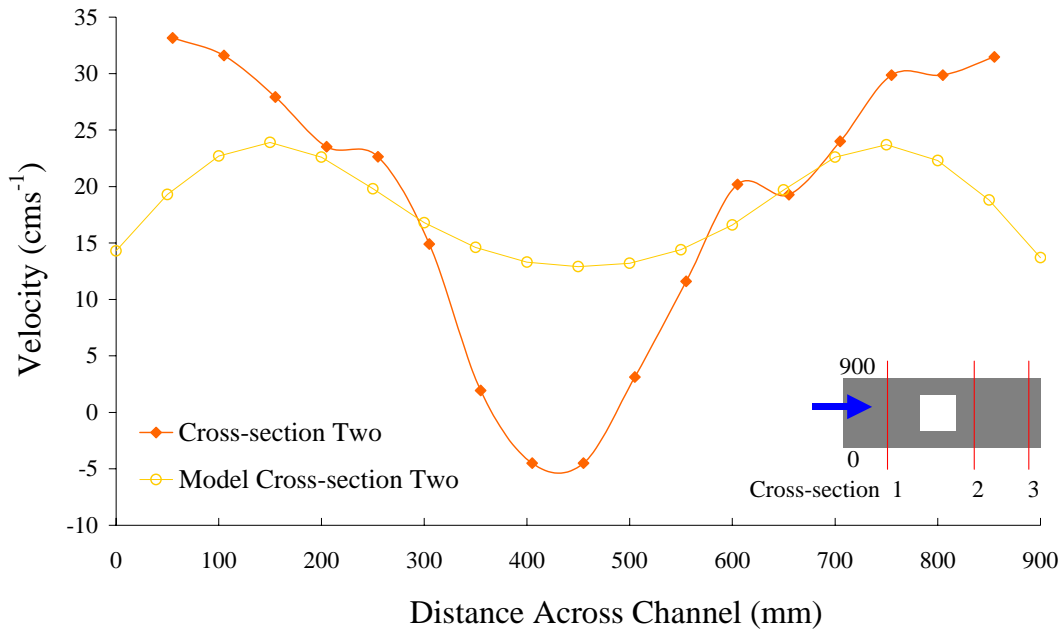


Figure 3.40 Comparison of depth averaged velocity field obtained from model morphology and that measured near the bed in laboratory Experiment One, immediately downstream of the obstruction.

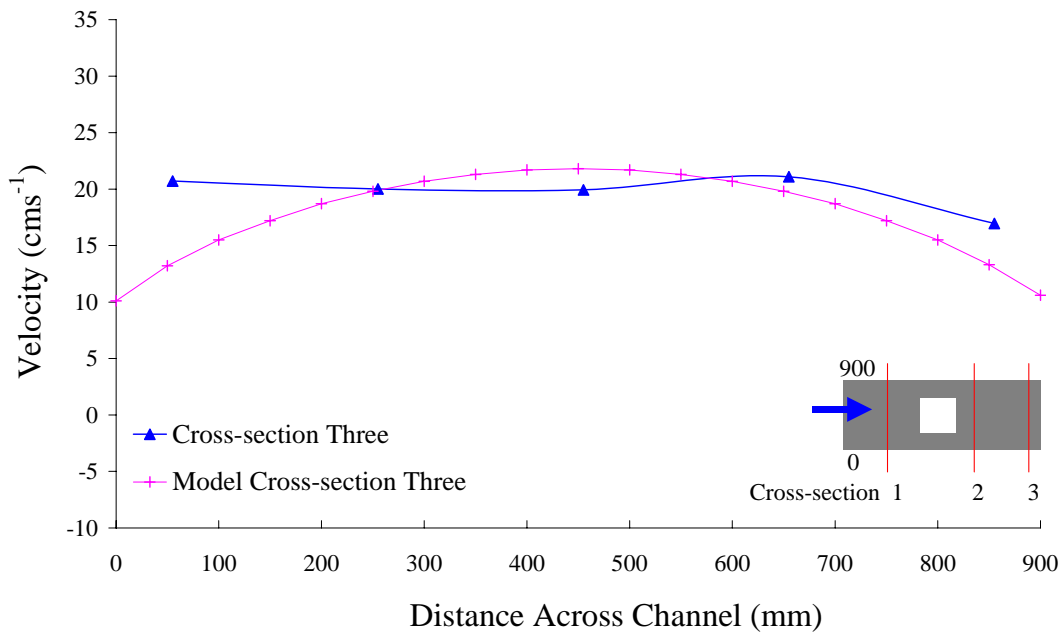


Figure 3.41 Comparison of Velocity field obtained from model morphology and that measured in laboratory Experiment One, down stream of the obstruction and deposition mounds.

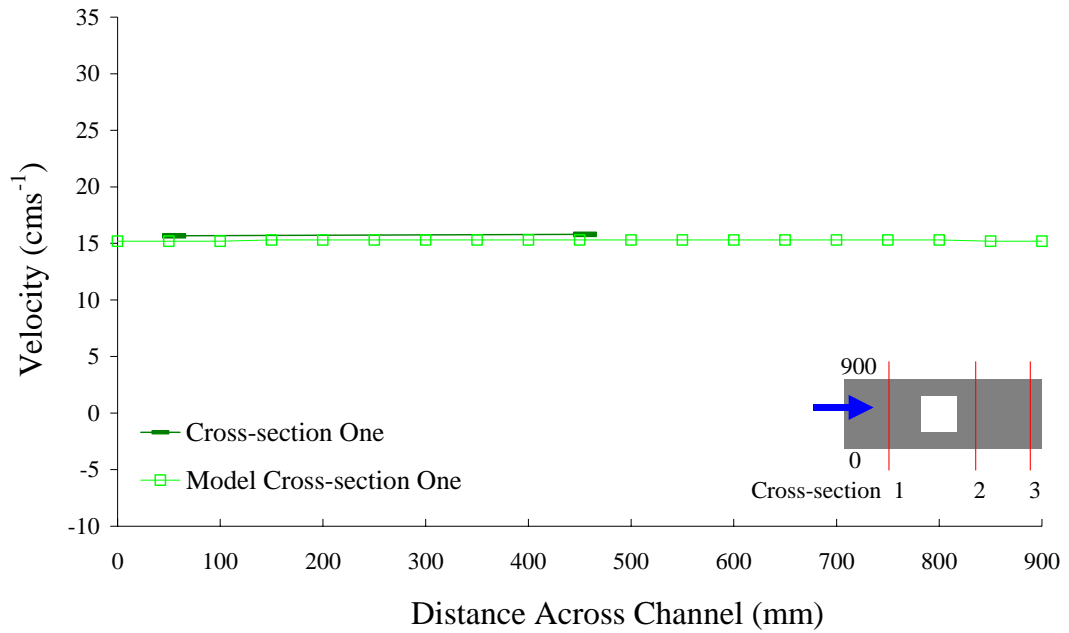


Figure 3.42 Comparison of depth averaged velocity field obtained from model morphology and that measured near the bed in laboratory Experiment Two, upstream of the obstruction.

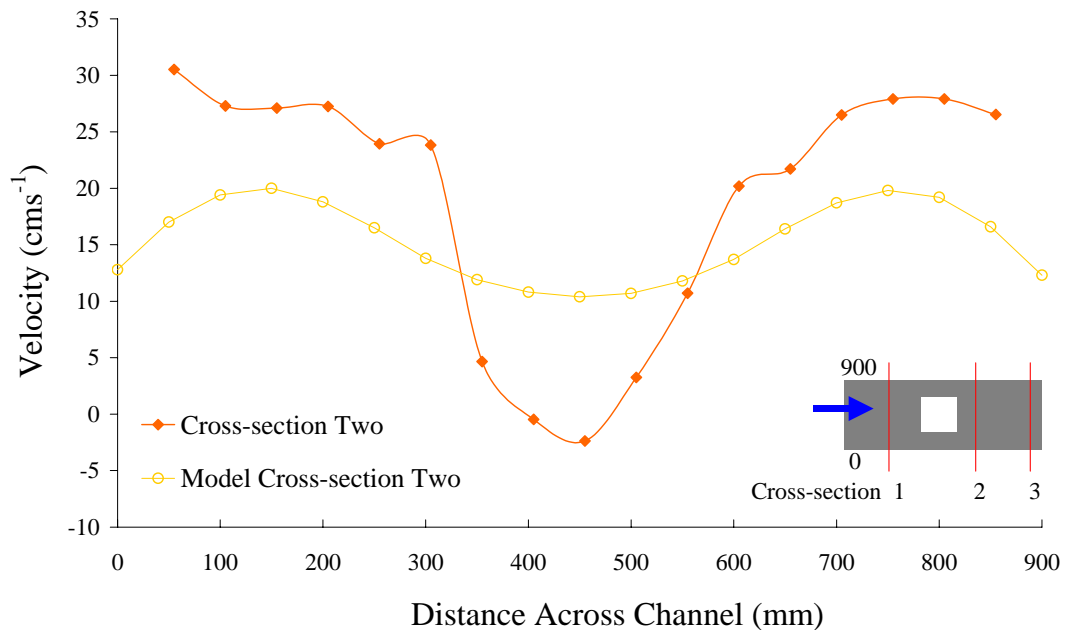


Figure 3.43 Comparison of depth averaged velocity field obtained from model morphology and that measured near the bed in laboratory Experiment Two, immediately downstream of the obstruction.

The third cross-section comparison shows that the model is unable to replicate the physical state, where the velocities become similar to those observed upstream of the obstruction. The measurement of the third cross-section was

further down stream than the morphological calculations, so the morphology used in the model to calculate the velocities had to be inferred which may have introduced some error into the calculation. Also the edge effects in the hydrodynamic model may have introduced some errors into the velocity calculations. Overall, an acceptable agreement was observed between the hydrodynamic velocity calculations and the laboratory measured velocities.

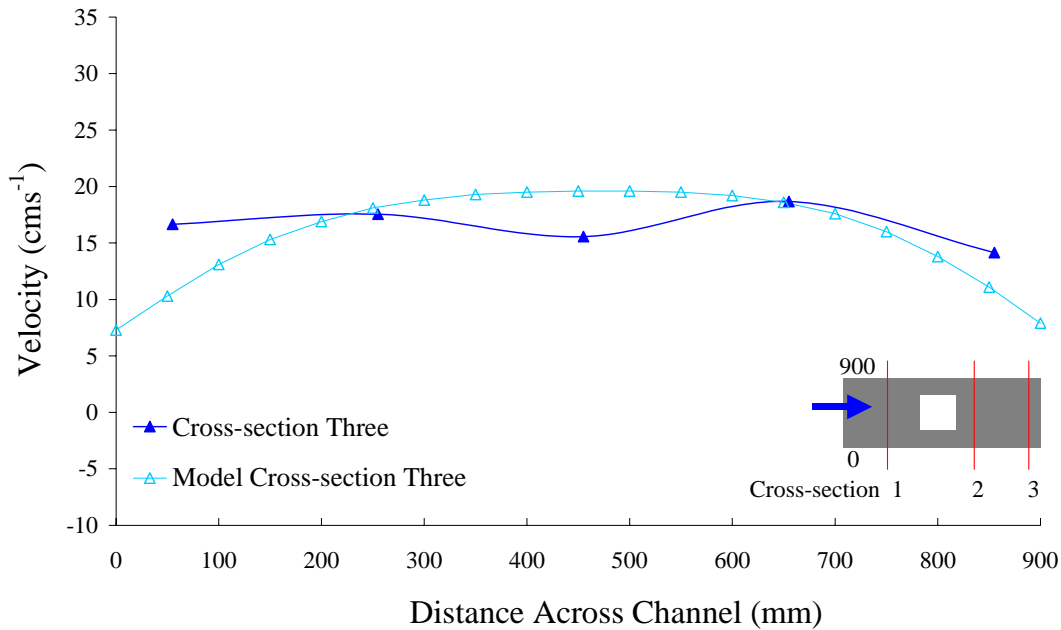


Figure 3.44 Comparison of depth averaged velocity field obtained from model morphology and that measured near the bed in laboratory Experiment Two, downstream of the obstruction and deposition mounds.

3.8.9 Conclusions

The cellular automata model represents the height and shape of the depositional mounds better than the conventional model as a comparison of Brier Skill Scores shows, but more importantly is a different way to determine equilibrium morphologies.

The cellular automata model also represents a reduced computation time, with run times for an average model less than a quarter of an average traditional model run when a similar grid size was used.

The cellular automata model differs from other self-organisation-based coastal models such as Werner and Fink (1993) or Coco et al. (2004) as it predicts a single stable equilibrium morphology formed around an obstruction or constriction, similar to multiple rock obstructions in the study by Jiménez-

Hornero et al. (2003). However, their model looked at runoff events where as the model discussed in the previous sections analyses river flow around a single, rather than multiple obstructions.

3.9 Unidirectional Lagoon Example

Up until this point, only small-scale laboratory examples have been discussed. This Section expands upon this foundation, using the same cellular automata structured model detailed in Section 3.1, to apply self-organisation techniques to a unidirectional lagoon/inlet type problem that has a scale of kilometres rather than metres.

3.9.1 Case Study Definition

The modelled simplified lagoon consists of a non sloping, moveable bed 1.3km by 0.5km in size, with fixed bed entrance and exit channels. These are fixed to allow comparisons to be made between different morphologies and to simplify the calculation of energy dissipation over the system. The models use grid cells that are 50m by 50m in size. This means that the moveable bed consists of an area 25 by 9 grid cells in size. The fixed bed areas consist of 20 grid cells each. Only the erodible lagoon is of interest as far as the development of an equilibrium stable morphology is concerned. In the idealised study discussed in this Section, only unidirectional flow is considered. Reversing flow is modelled in the following Chapter in Section 4.4, using the entropy based model. Flow enters the lagoon with a velocity of 0.8ms^{-1} . The entering flow is prescribed a sediment concentration of zero in this simplified case study, mimicking a situation where barrages control water flow from an upstream river or lake. A pictorial description of the likely erosional channel and depositional mound in the system is shown in Figure 3.45.

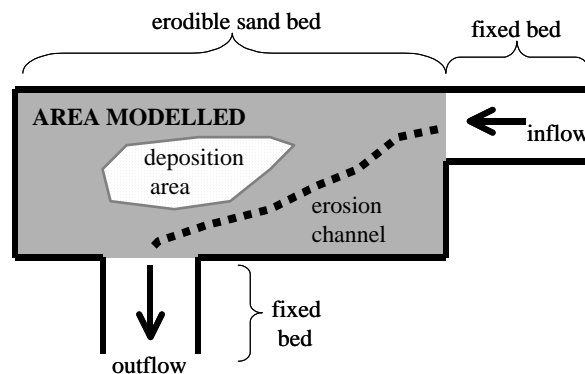


Figure 3.45 System layout for prediction of lagoon equilibrium morphology.

3.9.2 Results and Discussion

The resultant morphology of the self-organised lagoon system can be seen in Figure 3.46. The darker areas represent a channel that has formed between the entrance to the shallow tidal area and the exit of the flow to the open ocean. Some of the sand eroded from the channel has been deposited in the less energetic area downstream of the flow entrance (the lighter coloured areas), while some has been transported out of the analysed area. This result can be compared to the morphology of the Murray Mouth tidal lagoon, as shown in Figure 4.34, Chapter 4, Section 4.4.2.

The predicted morphology of the described model is comparable to the outcome of the study by de Boer (2001) on the use of a self-organisation based model to determine the morphology of a fluvial landscape. In the fluvial landscape study, a large-scale single pattern was predicted. The derived lagoon morphology in the current Section is also a large-scale single pattern in contrast to the small-scale rhythmic repetitive pattern of Pannell et al.'s (2002) ripples. However, the lagoon situation examined in this Section considers sand movement under water and therefore has some similarity in its rule definitions to the research of Pannell and his colleagues. Their rules considered small-scale movement and repetitive formations, while the research in this thesis is interested in larger scale movement and rearrangement around a fixed inflow and outflow channel.

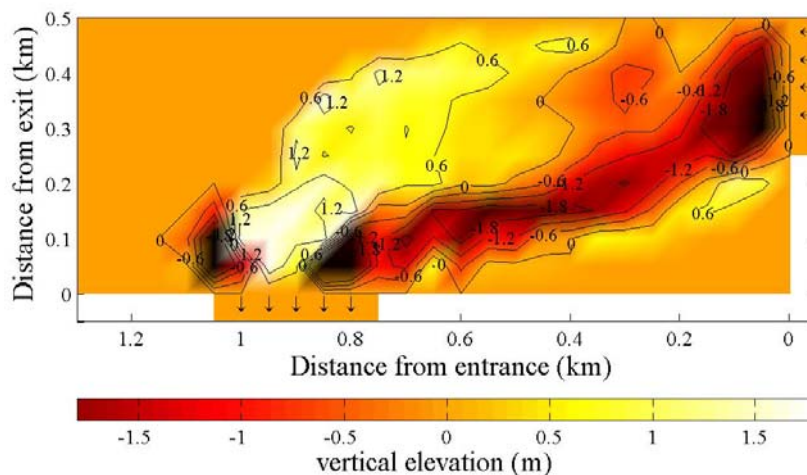


Figure 3.46 Resultant morphology from application of self-organisation-based method. Flow was from right to bottom.

The lagoon model differs from braided river cellular automata models such as the one proposed by Murray and Paola (1994), as it considers a wide, flat area, completely immersed in water, with flow entering and exiting from different sides of the lagoon area. In Murray and Paola's braided river study, water only enters

some cells and flow direction is determined by slope, while sediment is transported based on the Exner mass-balance equation, rather than the sediment increment-velocity ratio used in the lagoon cellular automata model. It differs from Coulthard and Macklin's (2003) contaminated sediment cellular automata model in a similar way. Their contaminated sediment model considers water runoff forming dendritic patterns over a vast area, rather than a more concise area submerged in water as in the lagoon model.

3.9.3 Energy Dissipation Trends – A Link to Entropy-Based Modelling

Energy dissipation was measured as the system moves towards equilibrium (see Chapter Four, Section 4.1 for an explanation of energy dissipation measurement). As portrayed in Figure 3.47, the global energy dissipation between the entrance and exit of the lagoon reduced as the system reorganised itself, suggesting that minimum rate of energy dissipation is a possible indicator of a system's attainment of equilibrium. Hergarten and Neugebauer (2001) observed a similar result when they applied a self-organisation based model to the formation of drainage networks and obtained similar formations to those derived by minimum energy expenditure methods. Past uses of minimum energy dissipation as an entropy-based indicator for a system reaching a state of equilibrium were discussed in detail in Chapter Two, Section 2.2.4.

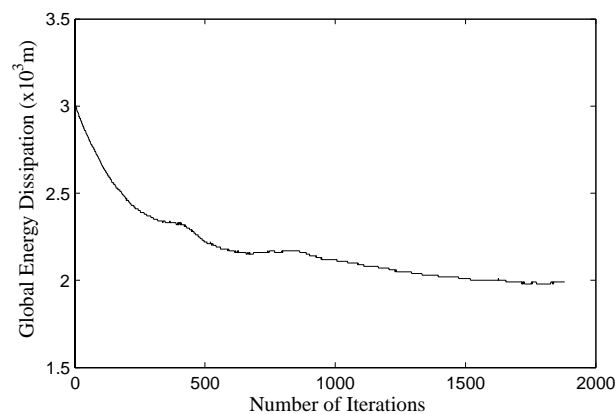


Figure 3.47 Global trend in energy dissipation as the lagoon system self-organises.

A similar result was obtained in the channel obstruction case study detailed earlier in this Chapter in Section 3.8. The results of reduction in energy dissipation over the system, as water moved around an obstruction in a channel, over a number of cellular automata model iterations are shown in Figure 3.48.

Similarly in river morphology it has been shown that the system will act to reduce or minimise the energy expenditure or energy loss from the system

between two river nodes or junctions. In this study the average difference in energy between the entry and exit of the channel in the model was observed, with a cross-section of the channel taken just upstream and downstream of the channel bounds for this analysis. As can be seen in the trend shown in Figure 3.48, as the system self-organised itself and moved towards a state of morphological equilibrium, the energy dissipation throughout the channel was reduced to a minimum value. The seemingly stepped profile, when viewed at a coarse scale is due to the fact that with minor sediment movement there is little effect of the overall flow field and hence energy loss at the beginning and end of the channel. At a point, a threshold is reached, and the effect of the morphology change then has a large effect on the energy at either end of the channel, swiftly affecting the global energy dissipation.

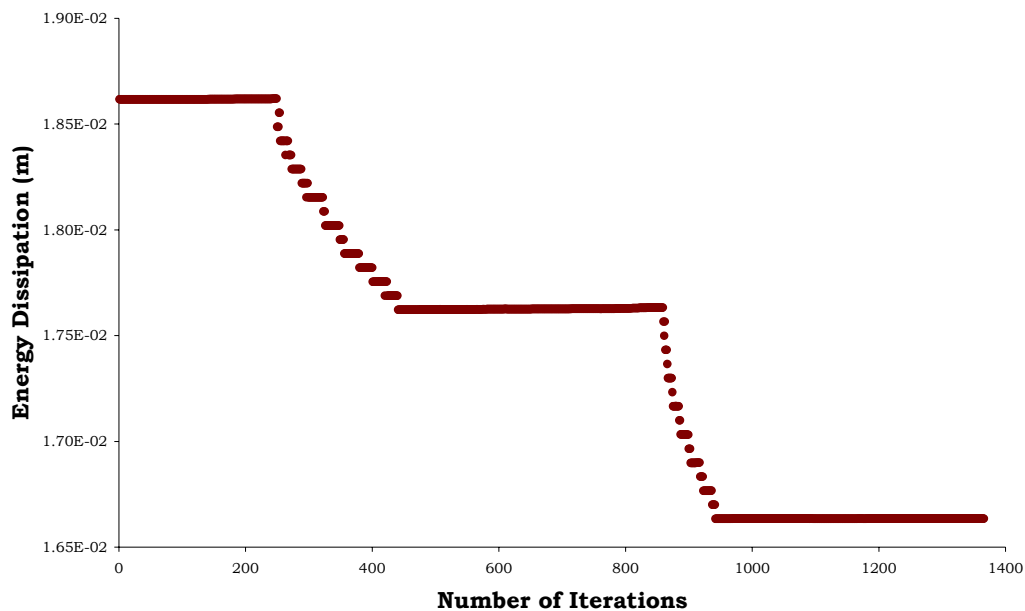


Figure 3.48 Global trend in energy dissipation as the channel obstruction system self-organises.

The use of energy dissipation as an indicator of equilibrium morphologies is discussed and described in the following Chapter. Some discussion and comparison between the entropy-based method and self-organisation-based methods is given in Chapter Four, Section 4.3.5.